1439

Université de Neuchâtel

Institut de chimie

Matériaux macromoléculaires du ferrocène: étude des relations structure-propriétés pour des polymères mésomorphes à chaînes latérales

Version réduite de la thèse présentée à la faculté des sciences de
l'Université de Neuchâtel pour l'obtention du titre de docteur ès science

par

François Turpin

Neuchâtel

1999

IMPRIMATUR POUR LA THÈSE

Matériaux macromoléculaires du ferrocène : étude des relations *structure-propriétés* pour des polymères mésomorphes à chaînes latérales

de M. François Turpin

UNIVERSITÉ DE NEUCHÂTEL
FACULTÉ DES SCIENCES

La Faculté des sciences de l'Université de Neuchâtel sur le rapport des membres du jury,

MM. R. Deschenaux (directeur de thèse), R. Tabacchi et D. Guillon (Institut de physique et chimie des matériaux, Strasbourg)

autorise l'impression de la présente thèse.

Neuchâtel, le 27 mai 1998

Le doyen:

F. Stoeckli

Liste des publications

Robert Deschenaux, Vladislav Izvolenski, **François Turpin**, Benoît Heinrich et Daniel Guillon, *Chem. Commun.* **1996**, 439.

Robert Deschenaux, **François Turpin** et Daniel Guillon, *Macromolecules* **1997**, *30*, 3759.

Robert Deschenaux, Isabelle Jauslin, Ulrich Scholten, **François Turpin**, Benoît Heinrich et Daniel Guillon, *Macromolecules* **1998**, *31*, 5647.

Robert Deschenaux, Florence Monnet, Elisabeth Serrano, **François Turpin** et Anne-Marie Levelut, *Helv. Chim. Acta* **1998**, *81*, 2072.

Ferrocene-containing thermotropic side-chain liquid-crystalline polymethacrylates

Robert Deschenaux,*[a] **Vladislav Izvolenski,**[a] **François Turpin,**[a] **Daniel Guillon**[b] **and Benoît Heinrich**[b]

[a] *Université de Neuchâtel, Institut de Chimie, Av. de Bellevaux 51, 2000 Neuchâtel, Switzerland*
[b] *Institut de Physique et Chimie des Matériaux de Strasbourg, Groupe des Matériaux Organiques, 23 Rue du Loess, 67037 Strasbourg Cédex, France*

The synthesis and mesomorphic properties of the title compounds, prepared by free-radical polymerization (or copolymerization) of a ferrocene-containing methacrylate monomer (with methylmethacrylate), are reported.

Metallomesogenic polymers represent an important field of current interest:[1] the combination of the properties of metals (polarisability, colour, magnetism) with those of polymers (processability) is expected to lead to anisotropic materials possessing unique characteristics which would be of particular interest for the design of new electro-optical devices.[1]

Recently we reported the first ferrocene-containing side-chain liquid-crystalline polymers which were synthesized by grafting vinyl-containing ferrocene momomers onto commercially available polyhydrosiloxanes.[2] The latter structures, which constituted the first liquid-crystalline polymers with appended organometallic units, showed high thermal stability, good solubility in organic solvents and broad enantiotropic mesophases. The observed results clearly demonstrated the great potential of ferrocene for elaborating polymeric architectures with essential properties.[1]

Obviously, better understanding and rationalization of the structure-mesomorphic properties relationship for ferrocene-containing liquid-crystalline polymers, and for metallomesogenic polymers in general, require the design and study of new systems.

Here we report the synthesis and thermal properties of the methacrylate-containing monomer **1** and of side-chain polymethacrylates **2a–f**, which were prepared by polymerization of **1** (→ **2a**) or by copolymerization of **1** with methylmethacrylate (MMA) (→ **2b–f**).

Monomer **1** was prepared following a step-wise procedure we developed for synthesizing unsymmetrically disubstituted ferrocene derivatives[3] (Scheme 1). Treatment of ferrocene-1,1′-dicarboxylic acid chloride **3**,[4] with phenol intermediate **4**[5] gave the mono-acid **5a** [purified by column chromatography (silicagel, CH_2Cl_2/AcOEt 10:1 and then CH_2Cl_2/AcOEt/AcOH 100:10:1) and crystallization (EtOH/CH_2Cl_2); mp = 176–178 °C], which was subsequently converted into the carboxylic acid chloride **5b** [purified by extraction of the solid residue with hot light petroleum (bp 90–120 °C); mp = 104–105 °C]. Esterification of **5b** with the methacrylate derivative **6**[6] furnished the targeted monomer **1** [purified by column chromatography (silicagel, CH_2Cl_2) and crystallization (EtOH/CH_2Cl_2)]. The structure and purity of compounds **1** and **3–6** were confirmed by elemental analysis and ^{1}H NMR spectroscopy.

Homopolymer **2a** and statistical copolymers **2b–f** were prepared by free radical polymerization of the appropriate monomer(s) [degassed THF, AIBN (1 mol% with respect to the overall monomeric concentration), 50 °C, 60 h, Ar], and were purified by column chromatography[7] (silicagel, CH_2Cl_2), precipitated by adding the concentrated CH_2Cl_2 solution to

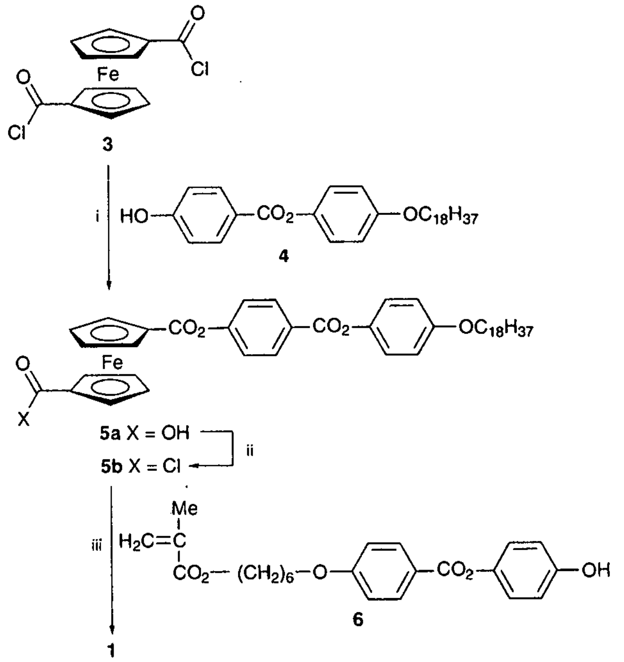

Scheme 1 *Reagents and conditions*: i, pyridine, benzene, reflux, 48%; ii, oxalyl chloride, pyridine, CH_2Cl_2, reflux, 98%; iii, Et_3N, CH_2Cl_2, reflux, 60%

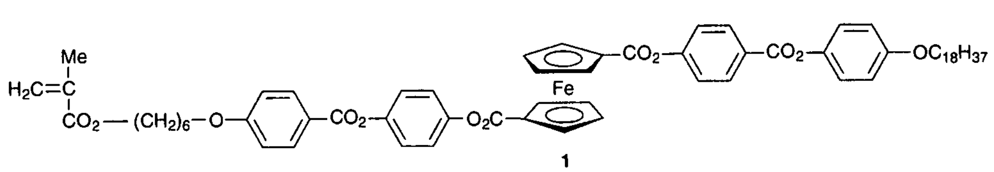

1

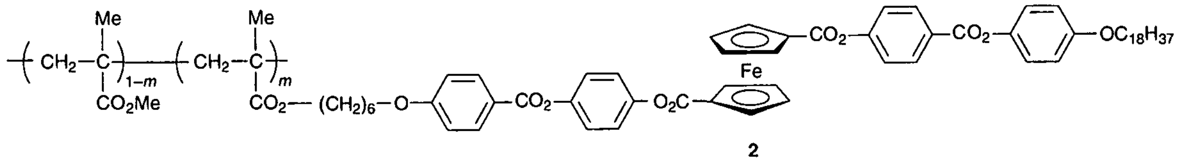

2

MeOH and finally recovered by centrifugation (60% yield). Removal of unreacted monomers and oligomers was confirmed by gel permeation chromatography (GPC) (see note *c* in Table 1).

The thermal and liquid crystal properties of monomer **1** and polymers **2a–f** were investigated by polarized optical microscopy, differential scanning calorimetry (DSC) and X-ray diffraction studies. The molecular weight and molecular weights distribution of **2a–f** were determined by GPC (see note *c* in Table 1). The data are listed in Table 1.

The ferrocene derivative **1** exhibited an enantiotropic smectic A phase (C·117·S_A·130·I) which was identified by polarized optical microscopy from the formation of a focal-conic fan texture and homeotropic areas. This was confirmed by X-ray diffraction analysis which revealed two sharp reflections (in a 2 : 1 ratio) in the small angle region and a diffuse band in the wide angle region.

Polymers characterized by a narrow molecular weights distribution (M_w/M_n ranged from 1.3 to 1.5) were obtained after purification. This is of particular interest in view of developing processable materials. All of the polymers showed good solubility in organic solvents such as $CHCl_3$, CH_2Cl_2, THF and toluene. The monomer content within the copolymers, analysed by ^1H NMR spectroscopy, was in agreement with the initial monomeric ratio in solution.

With the exception of **2f**, all of the polymers showed mesomorphic behaviour when examined by polarized optical microscopy. However, no typical textures were observed, either on heating or on cooling from the isotropic state. This is often the case for polymers due to their high viscosity.[8]

By DSC, the isotropization temperature could be determined for **2a–e**; reversible transitions were obtained from successive heating–cooling cycles. However, during the first heating run, the temperature at which the mesomorphic state formed (T_{LC}) was not apparent from the thermograms and, therefore, required X-ray diffraction investigations.

Table 1 Phase transition temperatures[a] and analytical data of polymers **2**

Polymer	x[b]	m[b]	M_n[c]	M_w[c]	M_w/M_n	T_g[d]/°C	T_{LC}[e]/°C	T_i[d]/°C
2a	1.00	1.00	74 800	111 300	1.5	30	100	210
b	0.90	0.88	63 400	81 700	1.3	40	105	201
c	0.80	0.78	47 500	60 500	1.3	40	105	192
d	0.60	0.58	57 000	75 800	1.3	40	105	176
e	0.40	0.38	42 000	53 000	1.3	40	105	143
f	0.10	0.12	64 300	99 500	1.5	80	101[f]	—

[a] Tg = glass transition temperature; T_{LC} = liquid-crystalline state formation; T_i = isotropization temperature. [b] x and m = molar fraction of monomer **1** in the feed and in the copolymers, respectively. [c] GPC data (THF, Ultrastyragel 10^3–10^4 Å, polystyrene standards). [d] DSC data (Mettler DSC 30 connected to a Mettler-TA 4000 processor; rate: 5 °C min^{-1}; under N_2; second heating run). [e] X-Ray data (transition obtained from the diffraction pattern registered with a curved counter 'Inel CPS 120' equipped with a bent quartz monochromator [Cu-Kα_1]; first heating run; approximate values). [f] Melting point (see text), determined by DSC from the first heating run.

X-Ray diffraction studies confirmed: (i) the liquid-crystalline character of polymers **2a–e**, (ii) the non-mesomorphic behavior of **2f** and (iii) revealed an amorphous character of **2a–e** below the liquid crystalline state during the first heating run.

In the case of **2a–e**, X-ray diffraction patterns gave two sharp peaks in the low-angle region (in a 2 : 1 ratio) and a diffuse peak in the wide-angle one. These data were consistent with the formation of disordered smectic phases (smectic C or smectic A phases). In order to gain further information about the nature of the mesophase(s), the *d*-layer spacing was determined as a function of temperature for **2a**: the *d*-layer spacing remained constant from 120 to 170 °C with an average value of 84.1 Å and then increased up to 89.5 Å near the clearing point. This behavior is an indication that **2a** might exhibit a smectic C phase. When cooled from the mesomorphic state to room temperature, **2a–e** solidified retaining the layered structure of the smectic phase. Therefore, the glass transition temperatures (Tg), which could be determined during the second heating run, corresponded to the transition between the glassy state and the liquid-crystalline phase.

The data reported in Table 1 emphasizes the role played by the MMA content in the polymeric structures. At low concentration, the MMA did not markedly influence the thermal properties of the polymers (compare **2a** and **2b**). An increase of the MMA concentration had no influence on the Tg and T_{LC} (compare **2b** and **2c–e**) but reduced the isotropization transition, the consequence of which was a reduction of the liquid-crystalline domain. This result was in agreement with the fact that **2f**, which contains 90% of MMA monomer, *i.e.* the highest percent of MMA of the described polymers, was found to be non-mesomorphic. Finally, polymers **2a–e** showed good thermal stability; no decomposition was observed in the liquid-crystalline state under the applied measurement conditions.

R. D. acknowledges the Swiss National Science Foundation (grant 20-39'485.93) for financial support and for a fellowship to F. T. and la Commission Fédérale des Bourses pour Etudiants Etrangers for a fellowship to V. I.

References

1 L. Oriol and J. L. Serrano, *Adv. Mater.*, 1995, **7**, 348, and references cited therein.

2 R. Deschenaux, I. Kosztics, U. Scholten, D. Guillon and M. Ibn-Elhaj, *J. Mater. Chem.*, 1994, **4**, 1351.

3 R. Deschenaux, M. Rama and J. Santiago, *Tetrahedron Lett.*, 1993, **34**, 3293; R. Deschenaux and J. Santiago, *Tetrahedron Lett.*, 1994, **35**, 2169.

4 F. W. Knoblock and W. H. Rauscher, *J. Polym. Sci.*, 1961, **54**, 651.

5 R. Deschenaux, J.-L. Marendaz and J. Santiago, *Helv. Chim. Acta*, 1993, **76**, 865.

6 S. B. Sastri and S. I. Stupp, *Macromolecules*, 1993, **26**, 5657.

7 U. Kumar, T. Kato and J. M. J. Fréchet, *J. Am. Chem. Soc.*, 1992, **114**, 6630.

8 *Side Chain Liquid Crystal Polymers*, ed. C. B. McArdle, Blackie, London, 1989.

Received, 2nd November 1995; Com. 5/07239E

Ferrocene-Containing Thermotropic Side-Chain Liquid-Crystalline Polymethacrylate from a Mesomorphic Trisubstituted Ferrocene Monomer

Robert Deschenaux* and François Turpin

Institut de Chimie, Université de Neuchâtel, Av. de Bellevaux 51,
2000 Neuchâtel, Switzerland

Daniel Guillon*

Institut de Physique et Chimie des Matériaux de Strasbourg, Groupe des Matériaux Organiques, 23 Rue du Loess, 67037 Strasbourg Cédex, France

Received January 13, 1997; Revised Manuscript Received April 8, 1997[⊗]

ABSTRACT: The synthesis and mesomorphic properties of a methacrylate-containing ferrocene monomer bearing two flexible chains at the 1,1′-positions and the corresponding side-chain homopolymer are described. Both polymer and monomer showed enantiotropic smectic C and smectic A phases. The liquid-crystalline phases were fully characterized by means of X-ray diffraction experiments. Dilatometric measurements pointed to a head-to-tail molecular arrangement of the monomeric units within the smectic A phase. The results described in this report confirm that ferrocene-containing thermotropic side-chain liquid-crystalline polymethacrylates respresent a valuable family of metallomesogenic polymers.

Introduction

Ferrocene-containing thermotropic side-chain liquid-crystalline polysiloxanes[1] and polymethacrylates[2] obtained from either 1,1′- or 1,3-disubstituted ferrocene derivatives form a valuable class of metallomesogenic polymers (metal-containing liquid-crystalline polymers):[3] both structures showed good thermal stability, good solubility in common organic solvents, and pronounced mesomorphic character (enantiotropic smectic C and/or smectic A phases). The above polysiloxanes represented the first metallomesogenic polymers with appended mesogenic organometallic units. The corresponding mesomorphic vinyl (→polysiloxanes) and methacrylate (→polymethacrylates) ferrocene monomers, comprising two aromatic rings at each substitution position, were synthesized following a stepwise procedure we developed for preparing unsymmetrically disubstituted low molar mass liquid-crystalline ferrocene derivatives.[4] Grafting of the vinyl-containing monomer onto commercially available polyhydrosiloxanes and free-radical polymerization of the methacrylate-containing monomer were performed following conventional, well-established, literature procedures.[1,2]

Liquid-crystalline behavior has also been observed for polyacrylates prepared from monosubstituted ferrocene monomers containing a biphenyl system as a rigid rod.[5] Direct comparison with our own compounds is not straightforward because very different structures have been investigated in these studies. However, narrower mesomorphic ranges were observed for homopolymers prepared from the monosubstituted ferrocene monomers.[5] This behavior is in agreement with results obtained with low-molar-mass compounds which showed that large organic rods are required for generating favorable intermolecular interactions to thwart the steric repulsions resulting from the presence of the bulky ferrocene core.[6]

Owing to its unique electrochemical properties,[7] ferrocene represents a unit of choice for developing electroactive mesomorphic polymers. Interestingly, we have recently shown that electron transfer can be used to induce mesomorphism in the ferrocene–ferrocenium redox system.[8]

The three-dimensional structure[9] of ferrocene offers multiple possibilities for forming monomeric derivatives. Structural modifications of the ferrocene core could be used for tuning the liquid-crystalline properties of the polymers. To reach this goal, a better undestanding of the *structure* (of monomers and polymers)–*mesomorphic behavior* relationship has to be provided. In other words, further structures should be prepared and studied.

The purpose of this report is to present the synthesis and characterization of a new methacrylate-based liquid-crystalline ferrocene monomer **1** and the corresponding homopolymer **I** (Chart 1). The 1,1′,3-substitution pattern was selected to explore the influence of polysubstitution on the thermal and mesomorphic properties of side-chain polymers. Compounds **1** and **I** represent the first trisubstituted ferrocene-containing monomer and polymer reported so far.

Results and Discussion

Monomer Synthesis. The synthesis of monomer **1** is outlined in Scheme 1. The key intermediate, the trisubstituted ferrocene derivative **5**, was prepared in three steps from ferrocene (**2**). Acylation of **2** with octanoyl chloride gave diacyl **3**, the reduction of which led to dialkyl **4**. Treatment of the latter with $POCl_3$ and DMF furnished aldehyde **5**, which was transformed into the carboxylic acid derivative **6** by reaction with malonic acid. Esterification of **6** with hydroquinone monobenzyl ether gave ester **7**. Hydrogenation of the latter under standard conditions led to phenol intermediate **8**, which was condensed with 4-(benzyloxy)benzoic acid to give benzyl derivative **9**. Removal of the benzyl protective group under standard hydrogenation conditions yielded phenol **10**. Finally, esterification of **10** with methacrylate derivative **11**[10] gave the targeted monomer **1**. The latter was purified by column chromatography (silica gel; eluent, CH_2Cl_2/AcOEt 50:1). Its purity and structure were confirmed by ^1H NMR spectroscopy, mass spectrometry, and elemental analysis.

[⊗] Abstract published in *Advance ACS Abstracts*, June 1, 1997.

Chart 1

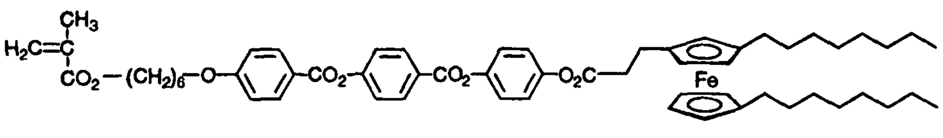

1

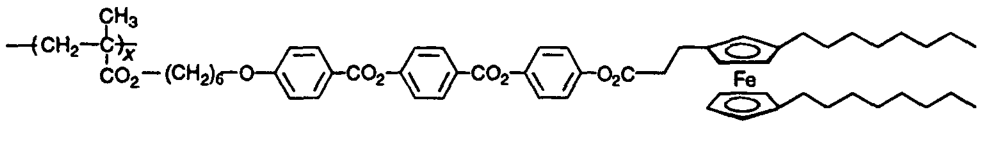

I

During the preparation of **5**, the 1,1′,2-trisubstituted derivative (see Chart 2) also formed in *ca.* 10% yield. The two isomers could be easily separated by column chromatography (silica gel; eluent, CH_2Cl_2/AcOEt 100:1): the 1,1′,2-trisubstituted ferrocene derivative eluted first followed by **5**. Their structures were identified by ^1H NMR spectroscopy (see Experimental Section) by analyzing the resonances of the three protons located on the disubstituted Cp ring. In the case of the 1,1′,3-isomer, protons $H_{2,4}$, which are *ortho* to the aldehyde function, are deshielded with respect to the one in the *meta* position (H_5). For the 1,1′,2-isomer, proton H_3, which is *ortho* to the aldehyde function, is deshielded with respect to the ones in *meta* positions ($H_{4,5}$). Additional proof was provided from NOESY experiments. For the 1,1′,2-isomer, a spatial coupling was observed between the proton of the aldehyde function and one proton of the CH_2 group connected to the Cp ring in position 1; as expected, this coupling was absent in the case of the 1,1′,3-isomer.

Polymer Synthesis. Polymer **I** was prepared in 61% yield by free-radical polymerization (THF, AIBN, 50 °C, 40 h, under argon) of monomer **1**. The polymer was purified by column chromatography (silica gel; eluent, CH_2Cl_2), as already described for other systems,[11] and precipitation in MeOH. The purity of **I** was confirmed by gel permeation chromatography (GPC), which revealed that unreacted monomer and oligomers were eliminated during the purification process. Polymer **I** was found to be soluble in common organic solvents such as THF, $CHCl_3$, and CH_2Cl_2. After purification, a polydispersity of 1.6 was obtained (Table 1).

Liquid-Crystalline Properties. The mesomorphic properties were investigated by a combination of polarized optical microscopy (POM), differential scanning calorimetry (DSC), and X-ray diffraction studies. The thermal and liquid-crystalline data of monomer **1** and polymer **I** are listed in Table 1.

Monomer. By DSC (second heating run), a T_g was obtained at −32 °C followed by an exotherm at 20 °C ($\Delta H = 22.9$ kJ mol^{-1}), indicating that cold crystallization occurred. Two endothermic peaks, indicative of mesomorphic behavior, were obtained at 32 and 88 °C.

Polarized optical miscroscopy supported the DSC data. Melting of the sample at 32 °C led to the formation of a smectic C phase, which transformed into a smectic A one at 55 °C. The transition at 88 °C corresponded to the isotropization temperature. No endotherm was detected by DSC at 55 °C, indicating a second-order character of the smectic C-to-smectic A transition. The mesophases were identified from their optical textures: the smectic C phase gave broken focal-conic and schlieren textures, and the smectic A phase presented a focal-conic texture and homeotropic areas.

The nature of the smectic C and smectic A phases was confirmed by X-ray diffraction analysis. Diffraction patterns typical of disordered smectic phases were recorded over the entire liquid-crystalline domain: a sharp diffraction peak was obtained at the small-angle region, and a diffuse one was detected at the wide-angle region.

Figure 1 shows the variation of the *d*-layer spacing as a function of temperature recorded on cooling the sample from the isotropic liquid. The *d*-layer spacing slightly increased from 52.0 (70 °C) to 52.5 Å (56 °C) and then decreased to 49.1 Å (30 °C). This behavior was in agreement with smectic A and smectic C phases.

From CPK molecular models, a molecular length L of *ca.* 49 Å was measured for **1** in the fully extended conformation. This value was significantly smaller than the *d*-layer spacing obtained within the smectic A phase (52.3 ± 0.2 Å at 60 °C).

To explain the discrepancy between the two values (49 and 52.3 Å), high resolution dilatometric measurements[12] were carried out, and the molecular area S, which represents the ratio between the molecular volume and the *d*-layer spacing, was determined (Figure 2): a value of 28.0 Å^2 was obtained at 60 °C.

Within the smectic A phase, the molecular area S is equal to σ (average molecular area in a plane perpendicular to the director) and corresponds to the bulkiness of the rigid core. A reasonable assumption for the molecular organization within the smectic A phase is to consider an alernate up and down packing (Figure 3). Thus, the area occupied by two aromatic cores should be the same as the one occupied by three aliphatic chains. Therefore, the experimentally determined σ value has to be compared to the transverse area of 1.5 fully stretched molten aliphatic chains leading to a σ value of $1.5 \times 21.9 = 32.9$ Å^2 (the value $\sigma = 21.9$ Å^2 was obtained at 60 °C from specific volume measurements in liquid paraffins[12−14] and verified for terephthal-bis(4-n-decylaniline)[15]). The discrepancy between the two areas (28.0 and 32.9 Å^2) means that the actual aliphatic sublayer thickness is larger than the length of the stretched chains, which implies that the position of neighboring rigid cores is shifted along the director. Such an organization leads to a calculated overall layer thickness of 53.2 Å,[16] which is in good agreement with the experimental value (see above).

The presence in the X-ray patterns of a diffuse reflection centered at ca. 10.0−10.5 Å, in addition to the one centered at *ca.* 4.5−5.0 Å, indicated the presence of a repetition distance which corresponded to two molecular rows within the layers; this result confirms the alternate up and down packing presented in Figure 3.

X-ray patterns (Figure 4) of a sample which could be oriented by crossing the isotropic-to-smectic A transition

Scheme 1[a]

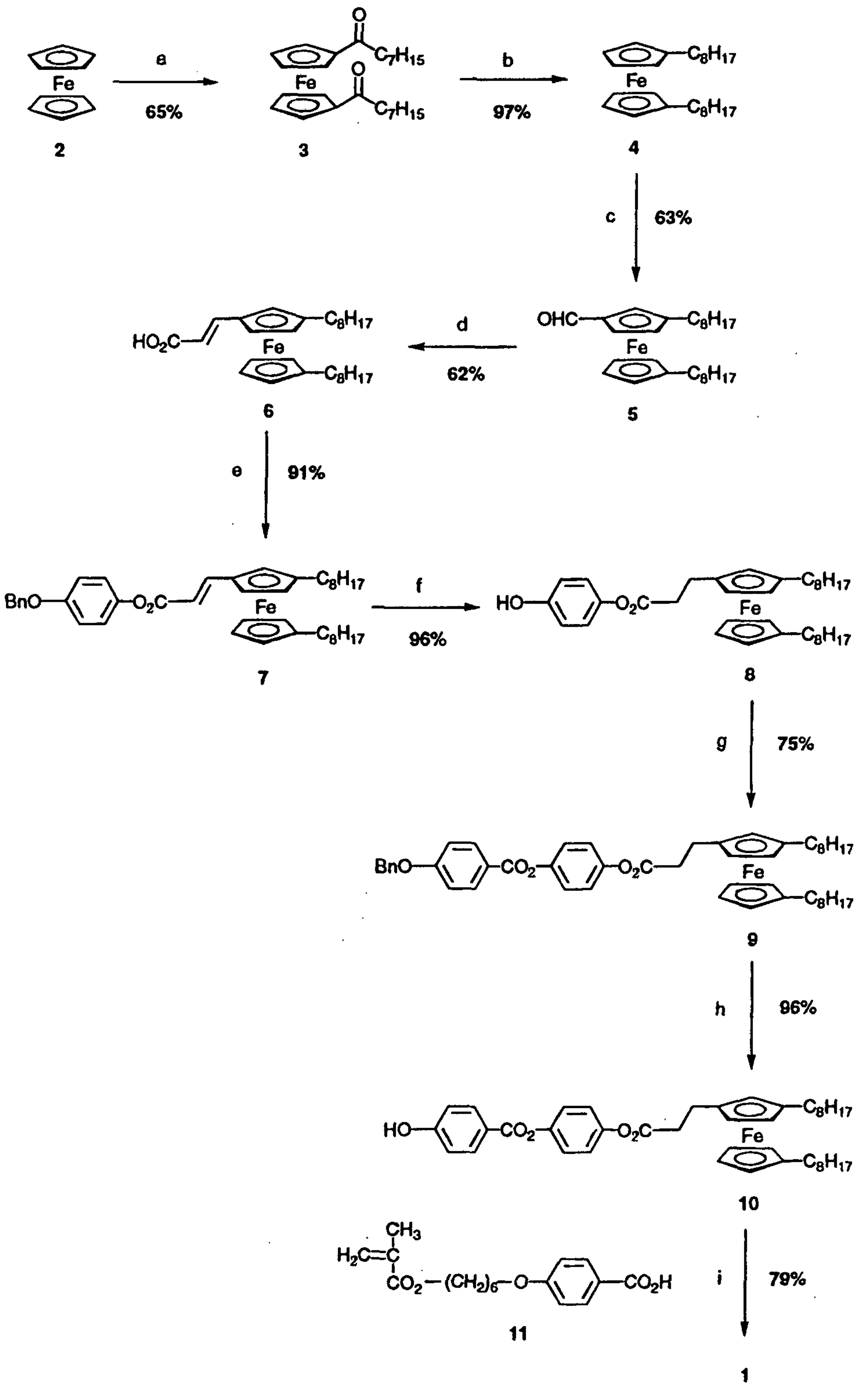

[a] (a) Octanoyl chloride, $AlCl_3$, CH_2Cl_2, reflux, 2 h. (b) $LiAlH_4$, $AlCl_3$, diethyl ether, 0 °C, 15 min. (c) DMF, $POCl_3$, CH_2Cl_2, reflux, 18 h. (d) Malonic acid, piperidine, pyridine, heat, 5.5 h. (e) Hydroquinone monobenzyl ether, *N,N'*-dicyclohexylcarbodiimide (DCC), 4-pyrrolidinopyridine (4-ppy), CH_2Cl_2, rt, 3 h. (f) H_2, Pd/C, CH_2Cl_2, rt, 10 h. (g) 4-(Benzyloxy)benzoic acid, DCC, 4-ppy, CH_2Cl_2, rt, 3 h. (h) H_2, Pd/C, CH_2Cl_2, rt, 20 h. (i) DCC, 4-ppy, CH_2Cl_2, rt, 3 h.

in a magnetic field of 1.4 T confirmed that both diffuse reflections corresponded to repetition distances within the layers (the arcs and circles being respectively the 4.5–5.0 and 10.0–10.5 Å reflections described above). By crossing the smectic A-to-smectic C transition, the director remained aligned in the field direction and the layer normal tilted from it. The tilt angles (ψ) could be determined from the X-ray pattern of the oriented sample; the values obtained were in agreement with those determined through the relation $\cos \psi = d_C/d_A$, d_C and d_A being the layer spacings in the smectic C and smectic A phases obtained from a powder sample. The variation of ψ as a function of temperature is given in Figure 5.

Polymer. By DSC (second heating run), two endotherms were detected at 154 and 185 °C. On cooling, reversible transitions were obtained.

Observation of **I** by POM supported the DSC data. A birefringent and viscous melt appeared above *ca.* 100 °C, the optical texture of which transformed at 154 °C, leading to homeotropic areas. The transition at 185 °C

Table 1. Properties of the Investigated Monomer and Polymer

Monomer 1

phase transitions[a] (°C)			
T_g	K/S_c	S_c/S_A[b]	S_A/I
−32	32 (22.6)	55	88 (3.6)

Polymer I

analytical data[c]			phase transitions[a] (°C)		
M_w	M_n	M_w/M_n	T_g	S_c/S_A	S_A/I
100 000	63 000	1.6	d	154 (2.9)	185 (1.2)

[a] T_g = glass transition temperature, K = crystalline state, S_c = smectic C phase, S_A = smectic A phase, I = isotropic liquid; onset values taken from the second heating run; enthalpy changes of the monomer (in kJ mol^{-1}) and the polymer in J g^{-1}) are given in parentheses. [b] Determined by polarized optical microscopy. [c] Determined by gel permeation chromatography. [d] Not detected.

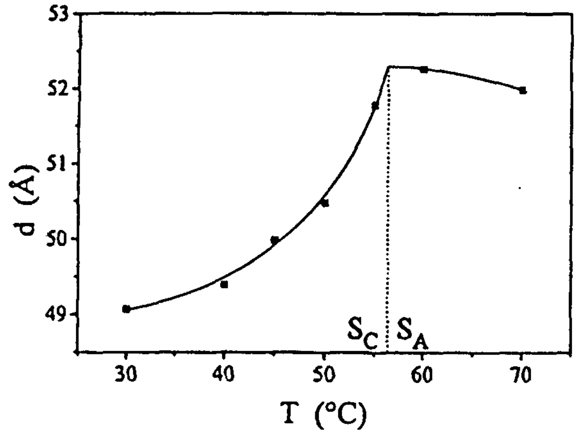

Figure 1. Variation of the *d*-layer spacing as a function of the temperature of monomer 1.

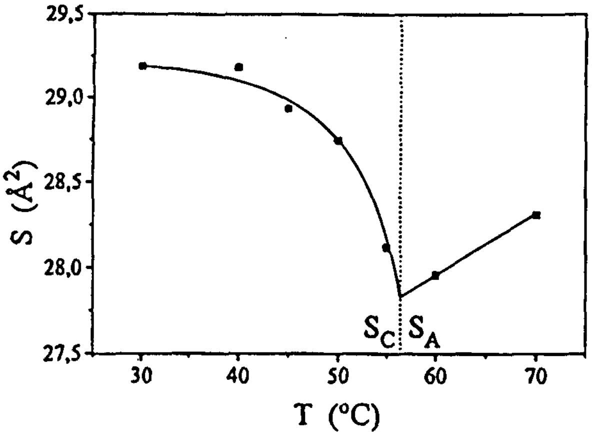

Figure 2. Variation of the molecular area as a function of the temperature of monomer 1.

corresponded to the clearing point. Therefore, POM indicated the formation of two liquid-crystalline phases (referred to as low- and high-temperature liquid-crystalline phase). When the sample was slowly cooled from the isotropic fluid, homeotropic and focal-conic textures were observed for the high-temperature liquid-crystalline phase, which was identified as a smectic A phase. Modification of the focal-conic texture was noticed on further cooling. However, the exact nature of the low-temperature liquid-crystalline phase could not be identified on the basis of POM examinations. This is often the case for viscous materials which do not allow typical liquid-crystalline textures to form.[17]

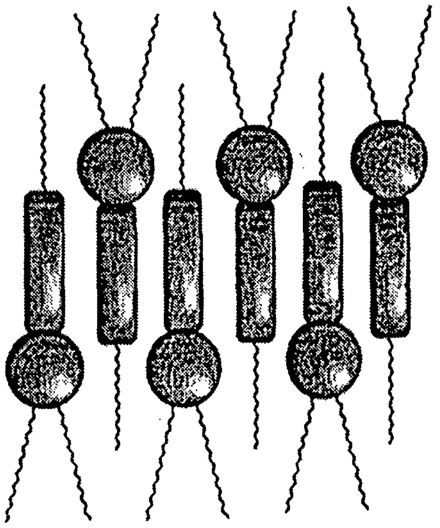

Figure 3. Schematic representation of the head-to-tail organization of monomer 1 within the smectic A phase.

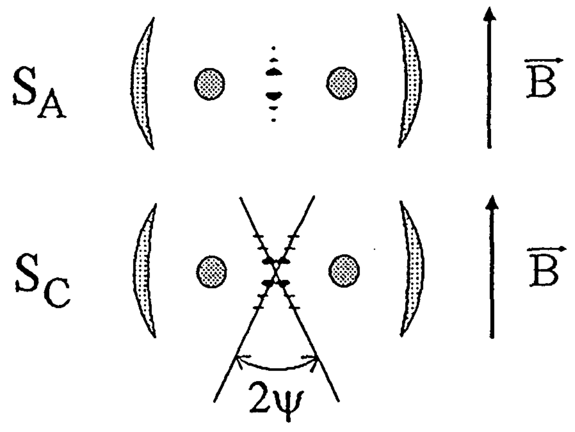

Figure 4. Schematics of the X-ray patterns obtained with an oriented sample of monomer 1 in the smectic A and smectic C phases ($\vec{B}$ is the direction of the magnetic field); see text for details.

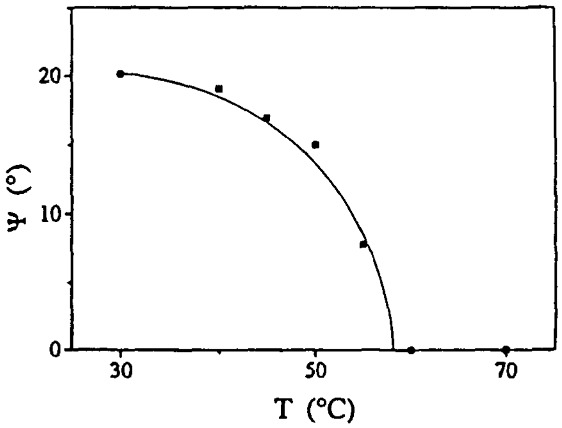

Figure 5. Variation of the tilt angle as a function of the temperature of monomer 1.

X-ray diffraction studies revealed a disordered smectic character for both mesophases: diffractograms consisting of two sharp peaks in the low-angle region and a diffuse one in the wide-angle region were recorded from 180 °C to room temperature. Therefore, the polymer retained the layered smectic organization at room temperature.

The variation of the *d*-layer spacing as a function of temperature was recorded on cooling the sample from the isotropic liquid (Figure 6). Two distinct regions were observed: the first one from the isotropic fluid to *ca.* 160 °C, in which the *d*-layer spacing increased to reach a maximum value of 67.5 Å, and a second one from 160

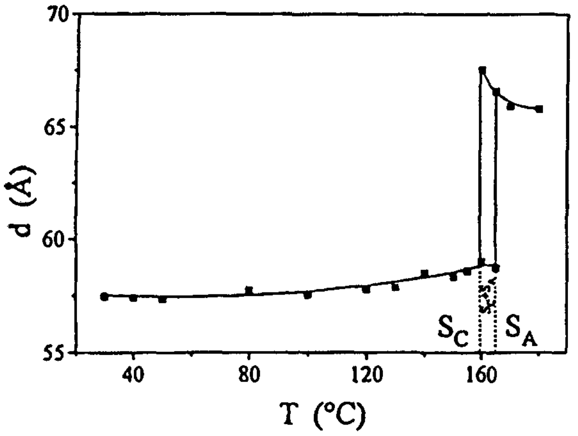

Figure 6. Variation of the *d*-layer spacing as a function of the temperature of polymer **I**.

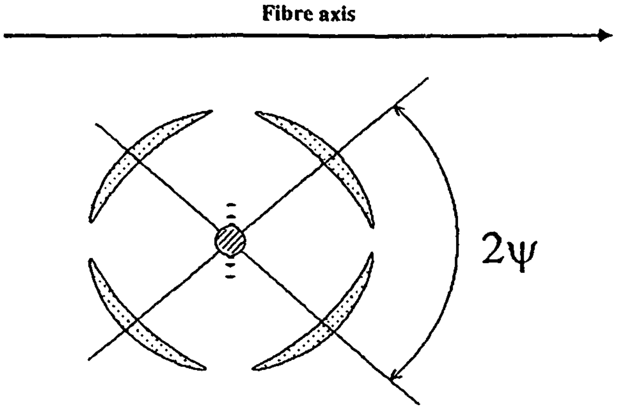

Figure 7. X-ray diffraction pattern of the smectic C phase of an oriented fiber polymer sample.

°C (59 Å) to 30 °C (57.5 Å), in which the *d*-layer spacing slightly decreased. The variation of the *d*-layer spacing indicated the presence of two smectic phases and confirmed the POM observations. Two *d*-values were obtained between 160 and 165 °C, revealing the coexistence of the two mesophases.

The temperature dependence of the *d*-layer spacing as a function of temperature strongly suggested that the low-temperature phase was smectic C in nature and the high-temperature phase was smectic A in nature. Contrary to monomer **1**, polymer **I** gave a first-order smectic C-to-smectic A transition.

The tilted nature of the low-temperature phase was confirmed from X-ray diffraction patterns recorded at room temperature for fibers pulled from the isotropic melt (near the clearing temperature) (Figure 7). The preferential stretching direction is parallel to the fiber axis and the layer normal perpendicular to the fiber axis. Consequently, the layer stacking reflections lie on a line perpendicular to the fiber axis and the diffuse reflections at *ca.* 4.5 Å lie on two lines tilted with respect to the fiber axis by the tilt angle between the director and the layer normal. Unfortunately, because of disorientation phenomena, no fiber patterns could be obtained above 80 °C.

Finally, the thermal stability of **I** was investigated by thermogravimetry. No decomposition was detected up to *ca.* 300 °C. Weight loss of 1, 5, and 10% was determined at 325, 345, and 352 °C, respectively.

The results described in the present report are of particular interest considering the current attention devoted to metallomesogenic polymers[3] and, in a more general sense, metallomesogens.[6,18] Firstly, a simple and efficient synthetic route was developed to synthesize 1,1′,3-trisubstituted ferrocene-containing liquid-crystalline monomers. Owing to the numerous substituents which can be used to derivatize the ferrocene unit,[6] such a substitution pattern leads the way to novel and most promising structures. Secondly, as compared to a previously published 1,1′-disubstituted methacrylate-containing ferrocene monomer (K/S_A, 117 °C; S_A/I, 130 °C),[2] compound **1** shows mesomorphic behavior near room temperature and a broad anisotropic range. This interesting combination of thermal and liquid-crytalline behavior is a consequence of the association of two flexible alkyl chains, which decrease the crystallization tendency, with a large organic rod, the presence of which is indispensable to thwart the steric repulsions of the bulky, three-dimensional, ferrocene core. Depression of transition temperatures consequent to the attachment of an alkyl chain to a ferrocene nucleus bearing a rigid organic rod was already observed (compare the thermal properties of monosubstituted ferrocene derivative **32** with those of corresponding alkyl derivatives **33** and **34** in ref 19) and is therefore in agreement with our own observations.

Polymer **I** has essential properties (good solubility in common organic media, good thermal stability, pronounced mesomorphic tendency) and makes such a structure an interesting material. The incorporation of **1** into a polymeric stucture strongly stabilized the liquid-crystalline phases (compare the clearing points of **1** and **I**). This result is in agreement with literature data.[20]

The results obtained for monomer **1** and polymer **I** and those we already reported[2] clearly prove that structural engineering can be used for tuning thermal and mesomorphic properties of ferrocene-containing monomers and related polymers. Finally, taking into account that the redox behavior of substituted ferrocene derivatives strongly depends on the nature and number of substitutents,[7] structural modifications can also be used to design mesomorphic polymers with tailor-made electroactive properties.

Conclusions

A trisubstituted methacrylate-containing mesogenic ferrocene monomer and the related side-chain liquid-crystalline homopolymer have been synthesized and their thermal and mesomorphic properties investigated by a combination of differential scanning calorimetry, polarized optical microscopy, thermogravimetry, and X-ray diffraction studies. Both monomer and polymer showed enantiotropic smectic C and smectic A phases. Owing to its three-dimensional structure, which offers multiple possibilities for forming derivatives by changing the nature, number, and position of the substituents, ferrocene is a promising organometallic unit for designing metallomesogenic polymers with tailor-made mesomorphic properties.

Experimental Section

Materials. Diethyl ether ($LiAlH_4$, under N_2), CH_2Cl_2 (P_2O_5, under N_2), and THF (sodium, benzophenone, under N_2) were distilled prior to use. Hydroquinone monobenzyl ether (Fluka, 99%), malonic acid (Fluka, 98%), *N*,*N*′-dicyclohexylcarbodiimide (Fluka, 99%), 4-pyrrolidinopyridine (Aldrich, 98%), anhydrous $AlCl_3$ (Fluka, 99%, puriss p.a.), $LiAlH_4$ (Fluka, 97%), DMF (SDS, analytical grade, 99.8%), $POCl_3$ (Fluka, 98%), octanoyl chloride (Fluka, 99%), and ferrocene (Chemische Betriebe Pluto/Veba Oel) were used as received. Pyridine (Fluka, 99.8%) and piperidine (Fluka, 99%) were stored on 4 Å molecular sieves. α,α′-Azoisobutyronitrile (Fluka, 98%) was crystallized from CH_3OH prior to use. 4-(Benzyloxy)benzoic acid was synthesized in two steps from methyl 4-hydroxybenzoate and benzyl bromide [(1) K_2CO_3, DMF, 120 °C for 3 h; crystallization from EtOH/THF. (2) Treatment in alkaline solution (KOH, EtOH/H_2O/THF), reflux, cooled to room temperature, acidified with HCl (5 N); crystallization from EtOH/hexane]. Methacrylate derivative **11** was synthesized following a literature procedure.[10]

Techniques. Column chromatography: silica gel 60 (0.060–0.200 mm, SDS). Transition temperatures (onset point) and enthalpies were determined with a differential scanning Mettler DSC 30 calorimeter connected to a Mettler TA 4000 processor, under N_2, at a rate of 10 °C min^{-1}; data treatment used Mettler TA72.2/.5 GRAPHWARE; for **1** and **I**, second heating run; for **3**, **7**, **9**, and **10**, first heating run. Thermogravimetry analyses were performed with a Mettler TG 50 thermobalance connected to a Mettler TA 4000 processor at a rate of 10 °C min^{-1}. Optical studies were conducted using a Zeiss-Axioscop polarizing microscope equipped with a Linkam-THMS-600 variable-temperature stage, under N_2. Gel permeation chromatography (GPC) was performed with a WATERS 510 instrument connected to a WATERS 410 differential refractometer (Ultrastyragel 10^3–10^4 columns calibrated with polystyrene standards; eluent, THF, 1 mL min^{-1}; T = 35 °C; treatment of data used Baseline 510 software). ^{1}H NMR spectra were recorded on a Varian GEMINI 200 spectrometer or a Bruker AMX 400 spectrometer, with the solvent as an internal standard. Mass spectra (chemical ionization, NH_3) were recorded on a Nermag R 30.10 spectrometer. Elemental analyses were done by Mikroelementaranalytisches Laboratorium ETH-Zurich or Ciba (Marly, Switzerland). Polymerization reactions were performed using Schlenk techniques under an inert Ar atmosphere.

X-ray Diffraction Studies. (a) Powder Samples. The crude powder was placed in Lindemann capillaries, and a linear monochromatic Cu-Kα beam obtained with a sealed-tube generator and a bent quartz monochromator was used. The diffraction patterns were registered either with a curved proportional detector "Inel CPS 120" or photographically. In general, the position of the second-order reflection in the small-angle region was used to determine the layer spacing. The temperature was controlled within ±0.05 °C.

(b) Oriented Samples. Fibers of the molten polymer were drawn (at a temperature close to the clearing point), bundled, and placed in a Lindemann capillary. For the monomer, the filled capillary was introduced into a magnetic field of 1.4 T and the sample was oriented by crossing many times the isotropic liquid-to-smectic A transition. The samples were illuminated by a pinhole Cu-Kα beam passing through a Ni-filter from a GX-20 Eliott rotating anode X-ray generator. The patterns were registered photographically, and the temperature was controlled within ±0.3 °C. Dilatometric measurements were performed with a high-precision home-made apparatus with an automatic computer-controlled operation, including data acquisition and temperature control within ±0.03 °C; relative variations of the specific volume could be detected with a resolution of 10^{-2}%, and its absolute value could be determined with an accuracy of 10^{-1}%.

Abbreviations. *N,N'*-Dicyclohexylcarbodiimide = DCC; 4-pyrrolidinopyridine = 4-ppy; dimethylformamide = DMF; α,α'-azoisobutyronitrile = AIBN.

Synthesis. 1,1'-Dioctanoylferrocene (3). A mixture of $AlCl_3$ (53.2 g, 0.40 mol) and octanoyl chloride (63.5 g, 0.39 mol) in CH_2Cl_2 (500 mL) was added to a stirred solution of ferrocene (**2**) (37.2 g, 0.20 mol) in CH_2Cl_2 (750 mL). The mixture was stirred under reflux for 2 h, cooled to room temperature, and poured onto ice. The organic layer was separated, dried ($MgSO_4$), and evaporated to dryness. Purification of the residue by column chromatography (hexane/AcOEt 10:1) and crystallization from hexane gave pure **3** (57.0 g, 65%). M_p = 60 °C. ^{1}H NMR (200 MHz, $CDCl_3$) δ 4.77 (t, 4 H, HCp), 4.48 (t, 4 H, HCp), 2.65 (t, 4 H, CH_2CO), 1.73–1.65 (m, 4 H, CH_2-CH_2CO), 1.59–1.31 (m, 16 H, aliphatic CH_2), 0.90 (t, 6 H, CH_3). Anal. Calcd for $C_{26}H_{38}O_2Fe$ (438.43): C, 71.23; H, 8.74. Found: C, 70.96; H, 8.62.

1,1'-Dioctylferrocene (4). To a suspension of $LiAlH_4$ (5.8 g, 0.15 mol) and diethyl ether (400 mL) cooled to 0 °C and kept under N_2 was added portionwise $AlCl_3$ (20.4 g, 0.15 mol). A solution of **3** (30.0 g, 0.068 mol) in diethyl ether (200 mL) was added. The mixture was stirred for 15 min and cautiously poured onto ice. The organic layer was separated and the aqueous phase extracted with diethyl ether. The organic layers were combined, washed successively with a saturated aqueous $NaHCO_3$ solution and a saturated aqueous NaCl solution, dried ($MgSO_4$), and evaporated to dryness. Purification of the residue by column chromatography (hexane) gave pure **4** (27.0 g, 97%, oil). ^{1}H NMR (200 MHz, acetone-d_6) δ 3.97 (s, 8 H, HCp), 2.35 (t, 4 H, CH_2Cp), 1.55–1.47 (m, 4 H, CH_2CH_2Cp), 1.30 (br s, 20 H, aliphatic CH_2), 0.89 (t, 6 H, CH_3).

1,1'-Dioctylferrocene-3-carboxaldehyde (5). To a solution of **4** (22.0 g, 0.054 mol) in CH_2Cl_2 (150 mL) heated under reflux was added dropwise a solution of $POCl_3$ (20.5 g, 0.134 mol) and DMF (17.4 g, 0.238 mol) in CH_2Cl_2 (50 mL). The solution was stirred under reflux for 18 h, cooled to room temperature, and poured onto ice. K_2CO_3 (80 g) was added portionwise, and the mixture was stirred for 1 h. Diethyl ether (100 mL) was added and the organic layer separated. The aqueous phase was extracted with diethyl ether (2 x 50 mL). The organic layers were combined, washed with water, dried (Na_2SO_4), filtered, and evaporated to dryness. Purification of the residue by column chromatography (CH_2Cl_2/AcOEt 100:1) gave pure **5** (15.0 g, 63%, oil). ^{1}H NMR (400 MHz, $CDCl_3$) δ 9.87 (s, 1 H, CHO), 4.61 (dd, J_o = 2.6 Hz, J_m = 1.3 Hz, 1 H, H_4), 4.58 (t, J_m = 1.3 Hz, 1 H, H_2), 4.42 (dd, J_o = 2.5 Hz, J_m = 1.5 Hz, 1 H, H_5), 4.09–4.04 (m, 4 H, HCp), 2.42–2.30 (m, 2 H, CH_2Cp(CHO)), 2.23 (m, 2 H, CH_2Cp), 1.56–1.48 (m, 2 H, CH_2-CH_2Cp(CHO)), 1.45–1.39 (m, 2 H, CH_2CH_2Cp), 1.37–1.25 (m, 20 H, aliphatic CH_2), 0.89 (t, 3 H, CH_3), 0.88 (t, 3 H, CH_3). MS: 439 (MH^+).

The 1,1',2-isomeric compound (first fraction) was isolated in *ca.* 10% yield (oil). ^{1}H NMR (400 MHz, $CDCl_3$) δ 10.03 (s, 1 H, CHO), 4.63 (m, 1 H, H_3), 4.42 (m, 1 H, H_4), 4.40 (m, 1 H, H_5), 4.08–4.05 (m, 4 H, HCp), 2.76–2.68 (m, 1 H, CH*H*Cp-(CHO)), 2.51–2.44 (m, 1 H, *C*HHCp(CHO)), 2.21 (m, 2 H, CH_2-Cp), 1.54–1.26 (m, 24 H, aliphatic CH_2), 0.88 (t, 6 H, CH_3). MS: 439 (MH^+).

Chart 2

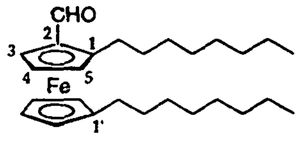

1,1',2-isomer

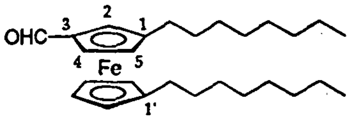

5

1,1',3-isomer

1,1'-Dioctylferrocene-3-*trans*-propenoic acid (6). A solution of **5** (12.0 g, 0.027 mol), malonic acid (4.2 g, 0.04 mol), and piperidine (25 drops) in pyridine (25 mL) was stirred at 55 °C for 4 h and at 110–120 °C for 1.5 h. The solution was poured onto a mixture of ice and water, and acidified with HCl (2 N). AcOEt was added and the organic layer separated, washed with H_2O, dried ($MgSO_4$), and evaporated to dryness. Purification of the residue by column chromatography (AcOEt) gave pure **6** (8.0 g, 62%, oil). ^{1}H NMR (200 MHz, $CDCl_3$) δ 7.62 (d, 1 H, vinylic proton), 5.96 (d, 1 H, vinylic proton), 4.32 (m, 2 H, HCp), 4.29 (m, 1 H, HCp), 4.01–3.94 (m, 4 H, HCp), 2.34 (m, 2 H, CH_2Cp(substituted by the vinylic function)), 2.22 (m, 2 H, CH_2Cp), 1.51–1.27 (m and br s, 24 H, aliphatic CH_2), 0.89 (t, 3 H, CH_3), 0.88 (t, 3 H, CH_3). MS: 481 (MH^+). Anal. Calcd for $C_{29}H_{44}O_2Fe$ (480.51): C, 72.49; H, 9.23. Found: C, 72.46; H, 9.40.

4-(Benzyloxy)phenyl 1,1'-Dioctylferrocene-3-*trans*-propenoate (7). A solution of **6** (4.0 g, 8.3 mmol), hydroquinone monobenzyl ether (2.0 g, 10 mmol), DCC (1.85 g, 8.96 mmol), and 4-ppy (0.13 g, 0.88 mmol) in CH_2Cl_2 (35 mL) was stirred at room temperature for 3 h. The mixture was filtered and evaporated to dryness. Purification of the residue by column chromatography (CH_2Cl_2) gave pure **7** (5.0 g, 91%). An analytically pure sample was obtained by crystallization from hexane. M_p = 63 °C. ^1H NMR (200 MHz, acetone-d_6) δ 7.67 (d, 1 H, vinylic proton), 7.53−7.33 (m, 5 H, aromatic protons, benzyl), 7.07 (m, 4 H, aromatic protons), 6.20 (d, 1 H, vinylic proton), 5.14 (s, 2 H, CH_2Ph), 4.56 (m, 2 H, HCp), 4.40 (m, 1 H, HCp), 4.09−3.98 (m, 4 H, HCp), 2.43 (m, 2 H, CH_2Cp-(substituted by the vinylic function)), 2.29 (m, 2 H, CH_2Cp), 1.61−1.30 (m and br s, 24 H, aliphatic CH_2), 0.89 (t, 3 H, CH_3), 0.87 (t, 3 H, CH_3). MS: 663 (MH^+). Anal. Calcd for $C_{42}H_{54}O_3Fe$ (662.73): C, 76.12; H, 8.21. Found: C, 76.28; H, 8.17.

4-Hydroxyphenyl 1,1′-Dioctylferrocene-3-propanoate (8). A mixture of **7** (4.8 g, 7.24 mmol), Pd(10%)/C (0.5 g), and CH_2Cl_2 (200 mL) was stirred at room temperature under 4.8 bar of H_2 for 10 h. The mixture was filtered and the solvent evaporated to dryness. Purification of the residue by column chromatography (AcOEt) gave pure **8** (4.0 g, 96%, oil). ^1H NMR (200 MHz, acetone-d_6) δ 8.40 (s, 1 H, OH), 6.94−6.80 (m, 4 H, aromatic protons), 3.99−3.94 (m, 7 H, HCp), 2.73 (m, 4 H, $CH_2CH_2CO_2$), 2.36 (t, 2 H, CH_2Cp), 2.32 (t, 2 H, CH_2Cp), 1.55−1.30 (m and br s, 24 H, aliphatic CH_2), 0.89 (t, 6 H, CH_3). MS: 575 (MH^+). Anal. Calcd for $C_{35}H_{50}O_3Fe$ (574.62): C, 73.16; H, 8.77. Found: C, 73.17; H, 8.85.

4-((4-(Benzyloxy)benzoyl)oxy)phenyl 1,1′-Dioctylferrocene-3-propanoate (9). A solution of **8** (4.0 g, 7.0 mmol), 4-(benzyloxy)benzoic acid (1.7 g, 7.4 mmol), DCC (1.54 g, 7.46 mmol), and 4-ppy (0.11 g, 0.74 mmol) in CH_2Cl_2 (100 mL) was stirred at room temperature for 3 h. The mixture was filtered and evaporated to dryness. Purification of the residue by column chromatography (CH_2Cl_2) and crystallization from CH_2Cl_2/EtOH gave pure **9** (4.1 g, 75%). M_p = 73 °C. ^1H NMR (200 MHz, acetone-d_6) δ 8.15 (d, 2 H, aromatic protons), 7.55−7.17 (series of m, 11 H, aromatic protons), 5.29 (s, 2 H, CH_2-Ph), 4.02−3.94 (m, 7 H, HCp), 2.78−2.72 (m, 4 H, $CH_2CH_2CO_2$), 2.38 (t, 2 H, CH_2Cp), 2.37 (t, 2 H, CH_2Cp), 1.55−1.31 (m and br s, 24 H, aliphatic CH_2), 0.88 (t, 6 H, CH_3). MS: 785 (MH^+). Anal. Calcd for $C_{49}H_{60}O_5Fe$ (784.86): C, 74.99; H, 7.71. Found: C, 75.02; H, 7.63.

4-((4-Hydroxybenzoyl)oxy)phenyl 1,1′-dioctylferrocene-3-propanoate (10). A mixture of **9** (4.0 g, 5.1 mmol) and Pd-(10%)/C (0.4 g) in CH_2Cl_2 (150 mL) was stirred at room temperature under 4.8 bar of H_2 for 20 h. The mixture was filtered and evaporated to dryness. Purification of the residue by column chromatography (CH_2Cl_2/AcOEt 10:1) and crystallization from hexane/EtOH gave pure **10** (3.4 g, 96%). M_p = 55 °C. ^1H NMR (200 MHz, acetone-d_6) δ 8.06 (d, 2 H, aromatic protons), 7.30 (d, 2 H, aromatic protons), 7.19 (d, 2 H, aromatic protons), 7.01 (d, 2 H, aromatic protons), 4.02−3.94 (m, 7 H, HCp), 2.90−2.72 (m, 4 H, $CH_2CH_2CO_2$), 2.38 (t, 2 H, CH_2Cp), 2.34 (t, 2 H, CH_2Cp), 1.55−1.31 (m and br s, 24 H, aliphatic CH_2), 0.88 (t, 6 H, CH_3). MS: 694 (M^+). Anal. Calcd for $C_{42}H_{54}O_5Fe$ (694.73): C, 72.61; H, 7.83. Found: C, 72.58; H, 7.82.

4-[[4-[[4-[[6-[(2-methyl-1-oxo-2-propenyl)oxy]hexyl]oxy]benzoyl]oxy]benzoyl]oxy]phenyl 1,1′-Dioctylferrocene-3-propanoate (1). A solution of **10** (3.1 g, 4.5 mmol), **11** (1.5 g, 4.9 mmol), DCC (1.03 g, 5.0 mmol), and 4-ppy (75 mg, 0.5 mmol) in CH_2Cl_2 (40 mL) was stirred at room temperature for 3 h. The mixture was filtered and evaporated to dryness. Purification of the residue by column chromatography (CH_2Cl_2/AcOEt 50:1) gave pure **1** (3.5 g, 79%). ^1H NMR (200 MHz, acetone-d_6) δ 8.29 (d, 2 H, aromatic protons), 8.16 (d, 2 H, aromatic protona), 7.53 (d, 2 H, aromatic protons), 7.38 (d, 2 H, aromatic protons), 7.22 (d, 2 H, aromatic protons), 7.14 (d, 2 H, aromatic protons), 6.07 (m, 1 H, vinylic proton), 5.61 (m, 1 H, vinylic proton), 4.18 (t, 2 H, CH_2O_2C or CH_2OPh), 4.16 (t, 2 H, CH_2O_2C or CH_2OPh), 4.02−3.94 (m, 7 H, HCp), 2.81−2.73 (m, 4 H, $CH_2CH_2CO_2$), 2.38 (t, 2 H, CH_2Cp), 2.34 (t, 2 H, CH_2Cp), 1.92 (m, 3 H, $CH_3C{=}C$), 1.91−1.71 (2 m, 4 H, CH_2-CH_2OPh and $CH_2CH_2O_2C$), 1.59−1.31 (m and br s, 28 H, aliphatic CH_2), 0.89 (t, 6 H, CH_3). MS: 982 (M^+), 983 (MH^+). Anal. Calcd for $C_{69}H_{74}O_9Fe$ (983.07): C, 72.08; H, 7.59. Found: C, 71.98; H, 7.51.

Preparation of Polymer I. A solution of monomer **1** (0.983 g, 1.0 mmol) and AIBN (1.64 mg, 0.01 mmol) in THF (5 mL) was stirred for 40 h at 50 °C in a thermostated bath. The solution was evaporated to dryness. Purification of the residue by column chromatography (CH_2Cl_2) and by precipitation from MeOH gave pure **I** (0.60 g, 61%), as a yellow solid. Anal. Calcd for $(C_{69}H_{74}O_9Fe)_n$: C, 72.08; H, 7.59. Found: C, 72.07; H, 7.59.

Acknowledgment. R.D. acknowledges the Swiss National Science Foundation for financial support (Grants Nos. 20-39485.93 and 20-45588.95) and Chemische Betriebe Pluto/Veba Oel AG, Germany, for a generous gift of ferrocene. We thank Dr. B. Heinrich for his assistance with X-ray and dilatometric experiments and for valuable discussions.

References and Notes

(1) Deschenaux, R.; Kosztics, I.; Scholten, U.; Guillon, D.; Ibn-Elhaj, M. *J. Mater. Chem.* **1994**, *4*, 1351.

(2) Deschenaux, R.; Izvolenski, V.; Turpin, F.; Guillon, D.; Heinrich, B. *Chem. Commun.* **1996**, 439.

(3) (a) Oriol, L. In *Metallomesogens*; Serrano, J. L. Ed.; VCH Verlagsgesellschaft: Weinheim, 1996; Chapter 5. (b) Oriol, L.; Serrano, J. L. *Adv. Mater.* **1995**, *7*, 348.

(4) (a) Deschenaux, R.; Kosztics, I.; Nicolet, B. *J. Mater. Chem.* **1995**, *5*, 2291. (b) Deschenaux, R.; Santiago, J. *Tetrahedron Lett.* **1994**, *35*, 2169. (c) Deschenaux, R.; Rama, M.; Santiago, J. *Tetrahedron Lett.* **1993**, *34*, 3293.

(5) Tanaka, H.; Hongo, T.; Hall, H. K. *Macromol. Rapid Commun.* **1996**, *17*, 91.

(6) Deschenaux, R.; Goodby, J. W. In *Ferrocenes: Homogeneous Catalysis, Organic Synthesis, Materials Science*; Togni, A., Hayashi, T., Eds.; VCH Verlagsgesellschaft: Weinheim, 1995; Chapter 9.

(7) Zanello, P. In *Ferrocenes: Homogeneous Catalysis, Organic Synthesis, Materials Science;* Togni, A., Hayashi, T., Eds.; VCH Verlagsgesellschaft: Weinheim, 1995; Chapter 7.

(8) Deschenaux, R.; Schweissguth, M.; Levelut, A.-M. *Chem. Commun.* **1996**, 1275.

(9) Elschenbroich, C.; Salzer, A. *Organometallics*; VCH Verlagsgesellschaft: Weinheim, 1992.

(10) Sastri, S. B.; Stupp, S. I. *Macromolecules* **1993**, *26*, 5657.

(11) Kumar, U.; Kato, T.; Fréchet, J. M. J. *J. Am. Chem. Soc.* **1992**, *114*, 6630.

(12) Allouchi, H.; Cotrait, M.; Guillon, D.; Heinrich, B.; Nguyen, H. T. *Chem. Mater.* **1995**, *7*, 2252.

(13) (a) Cruz, C.; Figueirinhas, J. L.; Sebastiao, P. J.; Ribeiro, A. C.; Noack, F.; Nguyen, H. T.; Heinrich, B.; Guillon, D. *Z. Naturforsch.* **1996**, *51a*, 155. (b) Guillon, D.; Heinrich, B.; Ribeiro, A. C.; Cruz, C.; Nguyen, H. T. Submitted for publication.

(14) Doolittle, A. K. *J. Appl. Phys.* **1951**, *22*, 1471.

(15) Guillon, D.; Skoulios, A.; Benattar, J. J. *J. Phys.* **1986**, *47*, 133.

(16) Calculated overall layer thickness: $[(1.5 \times 21.9/28.0) \times 24] + 25 = 53.2$ Å, where 24 Å represents the total length of the aliphatic chains of **1** and 25 Å represents the length of the rigid core of **1**. The 21.9 and 28.0 Å^2 values are explained in the main text.

(17) *Side Chain Liquid Crystal Polymers*; Mc Ardle, Ed.; Blackie: London, 1989.

(18) (a) *Metallomesogens: Synthesis, Properties and Applications;* Serrano, J. L., Ed.; VCH Verlagsgesellschaft: Weinheim, 1996. (b) Bruce, D. W. *J. Chem. Soc., Dalton Trans.* **1993**, 2983. (c) Bruce, D. W. In *Inorganic Materials*; Bruce, D. W., O'Hare, D., Eds.; Wiley: Chichester, 1992; Chapter 8. (d) Hudson, S. A.; Maitlis, P. M. *Chem. Rev.* **1993**, *93*, 861. (e) Espinet, P.; Esteruelas, M. A.; Oro, L. A.; Serrano, J. L.; Sola, E. *Coord. Chem. Rev.* **1992**, *117*, 215. (f) Giroud-Godquin, A.-M.; Maitlis, P. M. *Angew. Chem., Int. Ed. Engl.* **1991**, *30*, 375.

(19) Thompson, N. J.; Goodby, J. W.; Toyne, K. J. *Liquid. Cryst.* **1993**, *13*, 381.

(20) *Liquid-Crystalline Polymers*; Weiss, R. A., Ober, C. K., Eds.; ACS Symposium Series 435; American Chemical Society: Washington, DC, 1990.

MA970025R

Ferrocene-Containing Thermotropic Side-Chain Liquid-Crystalline Polysiloxanes

Robert Deschenaux,* Isabelle Jauslin, Ulrich Scholten, and François Turpin

Institut de Chimie, Université de Neuchâtel, Av. de Bellevaux 51, 2000 Neuchâtel, Switzerland

Daniel Guillon* and Benoît Heinrich

Institut de Physique et Chimie des Matériaux de Strasbourg, Groupe des Matériaux Organiques, 23 Rue du Loess, 67037 Strasbourg Cédex, France

Received March 16, 1998; Revised Manuscript Received June 11, 1998

ABSTRACT: The synthesis, purification, characterization, and liquid-crystalline properties of side-chain polysiloxanes bearing mesomorphic 1,1′- or 1,3-disubstituted ferrocene units are reported. The polymers were prepared by grafting the appropriate vinyl-containing ferrocene monomer onto commercially available poly(hydrosiloxane)s following a standard procedure. The monomers gave smectic A or smectic A and smectic C phases depending on the length of the flexible chains connected to the ferrocene unit. X-ray diffraction indicated that the polysiloxanes exhibited disordered smectic phases. Variation of the *d*-layer spacing determined for the polymers containing either 100% or 15–18% of the 1,1′-disubstituted ferrocene monomer (with the longest terminal alkyl chain) revealed the presence of smectic A and smectic C phases. Thermogravimetry showed a good thermal stability for the polymers.

Introduction

Side-chain liquid-crystalline polysiloxanes represent a class of interesting materials[1] which have found important applications in modern technology such as in the construction of information storage and ferroelectric devices[1,2] and in nonlinear optics.[3] These studies were made using organic homo- or copolymers. New developments may be expected by the introduction of a metal center into side-chain liquid-crystalline polysiloxanes. The combination of the properties of metals (color, polarizability, redox properties) with those of mesomorphic polymers (anisotropy, organization) seems particularly attractive for elaborating novel electrooptical devices.

If specific properties are to be exploited, the choice of the metal, and how it is connected to the polymeric structure, are of prime importance. Our interest in the search for new metallomesogens[4] based on organometallic frameworks[5–7] motivated us to consider ferrocene as a unit of choice for designing new metallomesogenic polymers.[8] Indeed, ferrocene-containing liquid crystals show good thermal stability, good solubility in common organic solvents, and, if appropriately substituted, high liquid-crystalline tendency.[5] Furthermore, the study of new metallomesogenic polymers will lead to important fundamental information to further explore and better understand the *structure–mesomorphic properties* relationship for such materials which are still in their infancy.

The successful development of unsymmetrically 1,1′- and 1,3-disubstituted mesomorphic ferrocene derivatives[9] provided an access to the synthesis of vinyl-containing ferrocene monomers. Grafting of these onto poly(hydrosiloxane)s following conventional and well-established procedures was expected to lead to the targeted polymers.

We report, herein, the synthesis, characterization and mesomorphic properties of vinyl-containing ferrocene monomers 1 and 2 (Chart 1) and of their corresponding side-chain polysiloxanes I and II (Chart 2). Preliminary results have already been communicated.[10] Prior to this report,[10] no side-chain liquid-crystalline polymers with appended mesomorphic organometallic units had been described.[8] Ferrocene derivative **1c** was selected to functionalize the poly(hydrosiloxane)s as it showed the highest liquid-crystalline tendency among the investigated monomers 1 (see below). As for monomer **2**, which led to higher melting and clearing points compared to the 1,1′-isomeric structure (see below), only a copolymer with a low ferrocene monomer content (15–18%) was synthesized; polymers with higher contents of the ferrocene moieties may exhibit too high clearing points and, consequently, decompose before reaching the isotropic liquid.

Chart 1

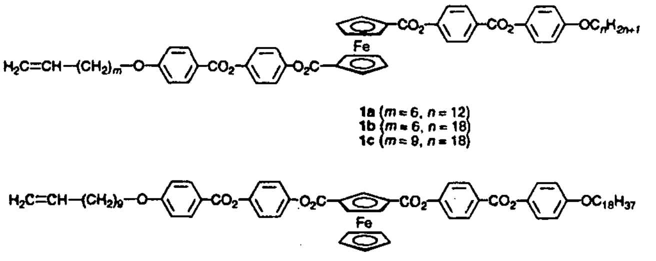

1a ($m = 6$, $n = 12$)
1b ($m = 6$, $n = 18$)
1c ($m = 9$, $n = 18$)

2

Results and Discussion

Monomer Synthesis. Monomers **1a–c** were prepared following the synthetic strategy described in Scheme 1. Ferrocene-1,1′-dicarboxylic acid chloride (**3**) was reacted with benzyl alcohol to give monoester **4**. Treatment of the latter with oxalyl chloride (→**5**) followed by condensation with phenol derivatives **6** (n = 12, 18) led to **7** (n = 12, 18). Removal of the benzyl protective group under standard hydrogenation conditions gave acids **8** (n = 12, 18), which were transformed with oxalyl chloride into the corresponding acid chlo-

S0024-9297(98)00410-0 CCC: $15.00

Chart 2

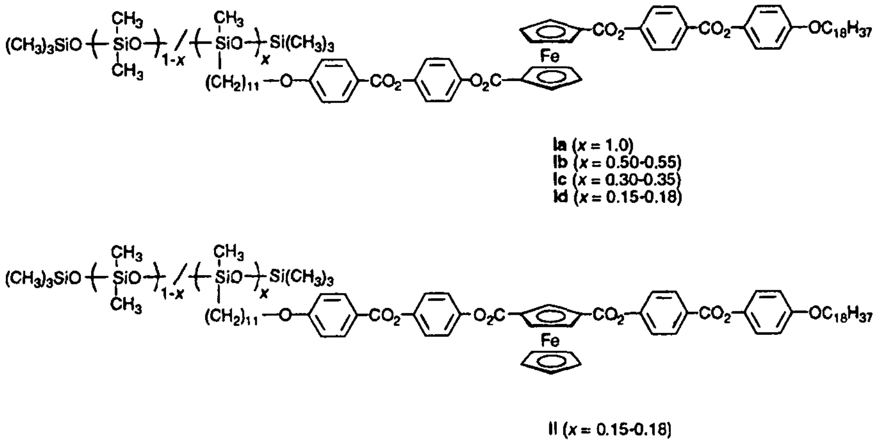

Scheme 1[a]

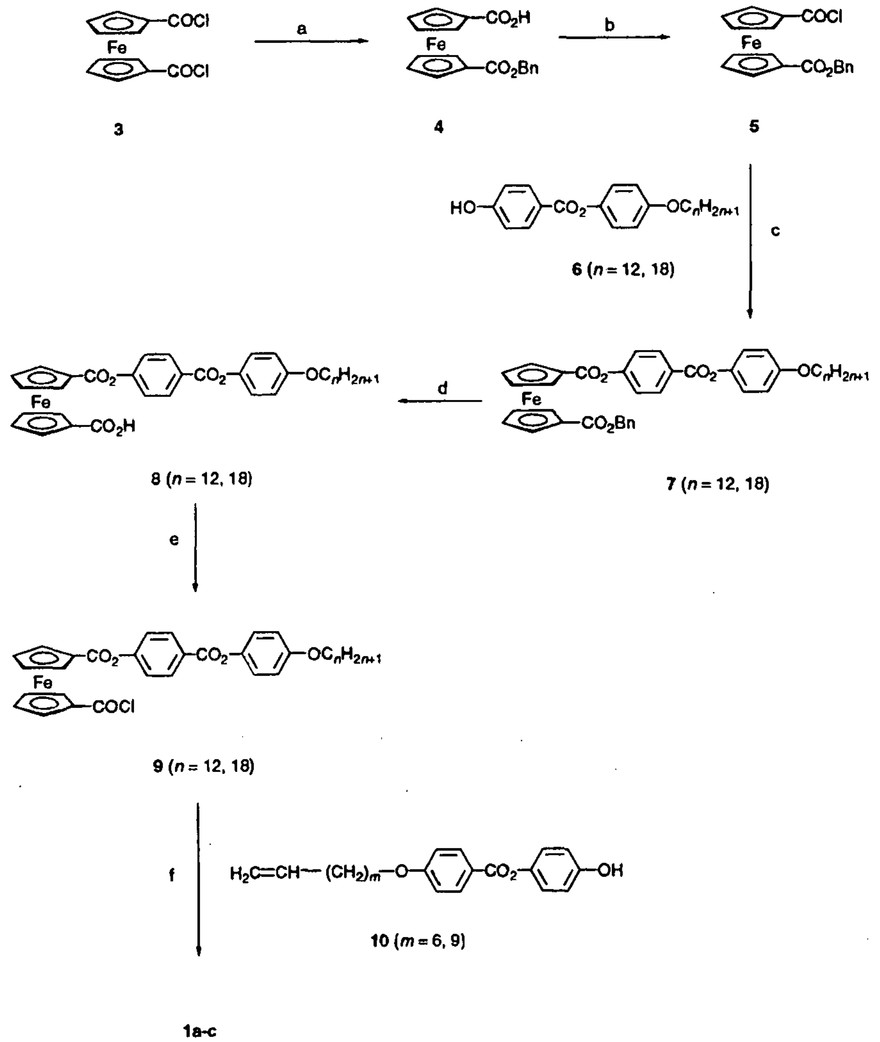

[a] Key: (a) benzyl alcohol, triethylamine, CH_2Cl_2, rt, 42%; (b) oxalyl chloride, pyridine, CH_2Cl_2, reflux, 100%; (c) Et_3N, CH_2Cl_2, reflux, 88% (for $n = 18$); (d) H_2, Pd/C, CH_2Cl_2/EtOH, rt, 87% (for $n = 18$); (e) oxalyl chloride, pyridine, CH_2Cl_2, reflux, 87% (for $n = 18$); (f) triethylamine, CH_2Cl_2, reflux, 70% (for **1c**, $m = 9$, $n = 18$).

rides **9** ($n = 12, 18$). Finally, esterification of **9** ($n = 12, 18$) with phenol derivatives **10** ($m = 6, 9$), containing the vinylic function, gave the targeted monomers **1a–c**.

Monomer **2** was prepared following the alternate procedure outlined in Scheme 2. Ferrocene-1,3-dicarboxylic acid chloride (**11**) was treated with phenol derivative **6** ($n = 18$) to give acid intermediate **12**, which was converted with oxalyl chloride to the corresponding acid chloride **13**. Condensation of the latter with **10** ($m = 9$) furnished the desired monomer **2**.

Polymer Synthesis. Polymers **Ia–d** and **II** were prepared by grafting either monomer **1c** (→**Ia–d**) or **2** (→**II**) onto the appropriate poly(hydrosiloxane) (**14a–d**) adapting a literature procedure[11] (Scheme 3). The progress of the reaction was monitored by following the decrease of the Si–H bond peaks by ^{1}H NMR (4.7 ppm, $CDCl_3$) and IR (2160 cm^{-1}) spectroscopy. Dissolution

Scheme 2[a]

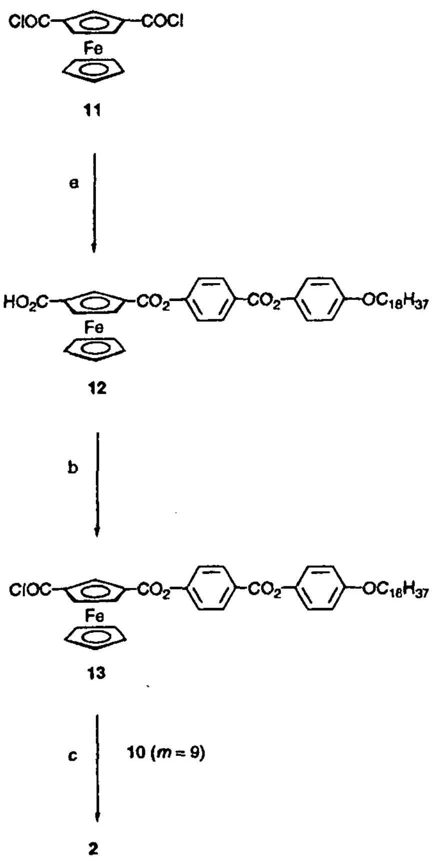

[a] Key: (a) benzene, **6** (n = 18, see Scheme 1), pyridine, reflux, 26%; (b) oxalyl chloride, pyridine, CH_2Cl_2, reflux, 84%; (c) CH_2Cl_2, **10** (m = 9, see Scheme 1), triethylamine, reflux, 62%.

Scheme 3[a]

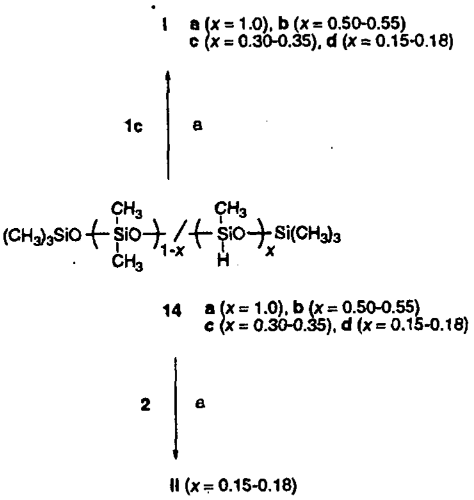

[a] Key: (a) toluene, $PtCl_2(1,5\text{-}C_8H_{12})$, 70 °C, 32% (for **Ia**).

Table 1. Molecular Weights and Molecular Weight Distributions of Investigated Polymers

polymer	molecular weight of starting polysiloxanes[a]	calcd molecular weight	% grafting[b]	M_w[c]	M_n[c]	M_w/M_n
Ia	2270	37 500	90	31 300	23 100	1.4
Ib	900–1000	max: 8800 min: 6400	100	26 100	18 600	1.4
Ic	2000–2100	max: 13 100 min: 10 800	100	29 700	20 400	1.5
Id	2000–2500	max: 9100 min: 6400	100	24 800	17 900	1.4
II	2000–2500	max: 9100 min: 6400	100	33 300	22 900	1.6

[a] Given by the supplier. [b] By ^{1}H NMR spectroscopy (see main text). [c] Data obtained by gel permeation chromatography.

Table 2. Phase Transition Temperatures and Enthalpy Changes of Investigated Monomers

monomer	transition[a]	T (°C)[b]	ΔH (kJ/mol)
1a	K → I	144	57.3
	(I → S_A)[c]	137	*d*
1b	K → S_A	135	55.0
	(S_C → S_A)[c,e]	117	
	S_A → I	145	10.8
1c	K → S_C	124	44.3
	S_C → S_A[e]	134	
	S_A → I	149	12.6
2	K → S_A	164	38.8
	(S_C → S_A)[c,e]	161	
	S_A → I	198	11.0

[a] K = crystalline state, S_C = smectic C phase, S_A = smectic A phase, I = isotropic liquid. [b] Note that the transition temperatures reported in our preliminary communication[10] (*i.e.* for **1c** and **2**) were determined on a Mettler DSC 30 calorimeter connected to a Mettler TA 3000 processor and corresponded to the peak transitions (see Experimental Section: Techniques). [c] Monotropic transition. [d] Not determined (peak overlap with the crystallization transition). [e] Determined by polarized optical microscopy.

of the crude material in CH_2Cl_2, precipitation with MeOH, and recovery by centrifugation led to pure polymers: Gel permeation chromatography (GPC) revealed that unreacted monomers and low-molecular weight oligomers were removed during the purification process.

The molecular weights (Table 1) of polymers **I** and **II** were determined, on one hand, by GPC and, on the other hand, by ^{1}H NMR spectroscopy taking into account the percent of substitution present in the starting polymer[12] (calculated by comparing the signal intensity of the methyl groups anchored onto the polymer backbone with that of the terminal CH_3 in the ferrocene-containing monomeric units) and the number of methylhydrosiloxane units (CH_3SiH).

The percentage of monomer grafting determined revealed that the reaction occurred with a good yield (90%) for homolymer **Ia** and quantitatively for copolymers **Ib–d** and **II**. With the exception of homopolymer **Ia**, the molecular weights calculated by NMR are smaller than those determined by GPC. This discrepancy arises from the fact that polystyrene standards were used to calibrate the GPC columns. The molecular weights obtained from both techniques cannot be compared.

Molecular weights distribution (M_w/M_n) (Table 1) ranging from 1.4 to 1.6 were obtained after purification.

Mesomorphic Properties. The mesomorphic properties were investigated by a combination of polarized optical microscopy (POM), differential scanning calorimetry (DSC), and X-ray diffraction (XRD). The thermal and liquid-crystalline data of the monomers (**1** and **2**) and polymers (**I** and **II**) are listed in Tables 2 and 3, respectively.

Monomers. Ferrocene derivative **1a** having the shortest flexible chains gave a monotropic smectic A phase. Monomer **1b** led to an enantiotropic smectic A phase and a monotropic smectic C one. As for **1c**, bearing the longest alkyl chains, it showed enantiotropic smectic C and smectic A phases. Ferrocene derivative **2** gave an enantiotropic smectic A phase and a monotropic smectic C one. Higher melting and clearing

Table 3. Phase Transition Temperatures of Investigated Polymers

polymer	transition[a]	T (°C)[b]	ΔH (J/g)	liq-crystalline behavior[a]
Ia	T_m	136	11.0	$S_C \to S_A$: 140 °C (by X-ray diffr)
	T_c	183	9.7	
Ib	T_m	127	9.4	smectic A phase (by X-ray diffr)
	T_c	173	8.4	
Ic	T_m	118	7.3	smectic A phase (by X-ray diffr)
	T_c	163	7.4	
Id	T_m	120	14.4	$S_C \to S_A$: 151 °C (1.4 J/g) (by DSC, polarized optical microscopy and X-ray diffr)
	T_c	159	1.4	
II	T_m	139	6.9	smectic A and/or smectic C phase(s) (by X-ray diffr)
	T_c	200	1.2	

[a] T_m = melting point, T_c = clearing point, S_C = smectic C phase, S_A = smectic A phase. [b] Note that the transition temperatures reported in our preliminary communication[10] (*i.e.* for **Ia** and **II**) were determined on a Mettler DSC 30 calorimeter connected to a Mettler TA 3000 processor (see Experimental Section: Techniques).

points were observed for **2** than for its isomeric analogue **1c**. The influence of the substitution pattern on the thermal properties can be explained from the X-ray crystal structure obtained for a 1,3-disubstituted ferrocene derivative,[13] which revealed that such a substitution pattern leads to a highly anisotropic structure compared to the "step" structure of ferrocene derivatives substituted in the 1,1′-positions.[14]

The liquid-crystalline phases were identified by POM. On cooling of the samples from the isotropic melt, textures typical of smectic A (focal conic fan texture and homeotropic areas) (for **1a–c** and **2**) and smectic C (broken focal conic fan and schlieren textures) (for **1b,c** and **2**) phases were observed.

The liquid-crystalline phases of **1c** and **2**, which were used for preparing the side-chain polysiloxanes **I** and **II**, were characterized by XRD. For both monomers, diffraction patterns typical of disordered smectic phases were recorded and showed two sharp reflection peaks (1:2 ratio) in the small-angle region and a diffuse band in the wide-angle region. The *d*-layer spacing was calculated for both monomers in the smectic A phase and was found to be 59.8 Å (at 135 °C) for **1c** and 57.1 Å (at 175 °C) for **2**. From CPK molecular models, a molecular length L of ca. 68.5 Å was measured for **1c** and **2** in their fully extended conformation. From these values, d/L ratios of 0.87 and 0.83 were obtained for **1c** and **2**, respectively. The discrepancy between the d and L values suggested a monomolecular organization of **1c** and **2** within the smectic A phase with a pronounced disorganization of the alkyl chains. Such an arrangement is in agreement with low-molar mass ferrocene-containing thermotropic liquid crystals we previously investigated.[15]

Polymers. All the polymers exhibited liquid-crystalline properties. Their melting and clearing points were determined by DSC and POM. Interestingly, polymer **Id** gave an additional endotherm which was indicative of the presence of two liquid-crystalline phases. Crystal-to-crystal transitions were detected for **Ia–c**. In the case of **Ia–c** and **II**, the liquid-crystalline phases could not be identified by POM. This is often the case for polymers owing to their viscosity which prevents the development of typical textures. In some cases, a focal-conic texture was observed and indicated a smectic nature of the liquid-crystalline phase(s). For **Id**, on cooling slowly the sample from the isotropic fluid, the formation of *bâtonnets*, which then transformed into a focal-conic fan texture, was clearly noticed. Homeotropic areas were also observed. On further cooling (i.e. after the second transition), a schlieren texture formed from the previous homeotropic areas, and the focal-conic fan texture transformed into a broken focal-conic fan texture. From these observations, the liquid-crystalline phases of **Id** were identified as smectic A (high-temperature mesophase) and smectic C (low-temperature mesophase) phases.

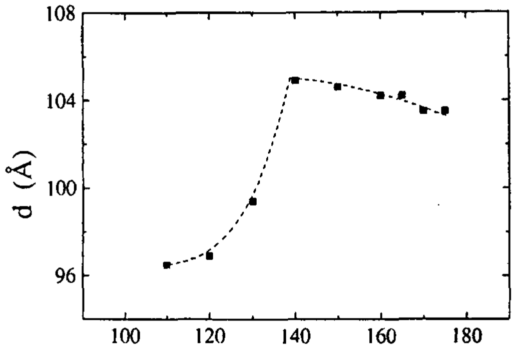

Figure 1. Variation of the *d*-layer spacing of polymer **Ia** as a function of temperature.[16]

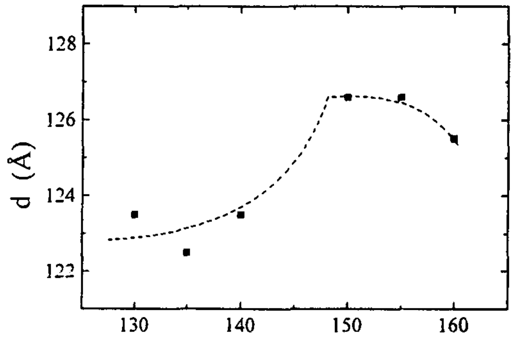

Figure 2. Variation of the *d*-layer spacing of polymer **Id** as a function of temperature.

Comparison of the melting and clearing points in series **I** and between **Id** and **II** showed the influence of the monomer content and structural isomerism on the thermal properties. First, decreasing the content of the mesogenic ferrocene monomer lowered both the melting and clearing points. Second, as expected from the results obtained for monomers **1c** and **2** (see above), incorporation of the 1,3-disubstituted ferrocene units onto the polymer led to a broadening of the liquid-crystalline domain.

The liquid-crystalline phases exhibited by **I** and **II** were investigated by XRD. Diffractograms typical of disordered smectic A and/or smectic C phases, characterized by two sharp diffraction peaks (1:2 ratio) in the low-angle region and a diffuse one in the wide-angle region, were recorded. The *d*-layer spacing was determined as a function of temperature for **I** on cooling the sample from the isotropic melt. For **Ia** (Figure 1) and **Id** (Figure 2), the variation of the layer thickness showed two regimes typical of smectic A (high-temperature liquid-crystalline phase) and smectic C (low-temperature liquid-crystalline phase) phases. These data supported the POM observations in case of **Id**. For **Ib,c**, the layer spacing was found to be nearly independent of temperature (not shown here) indicating that

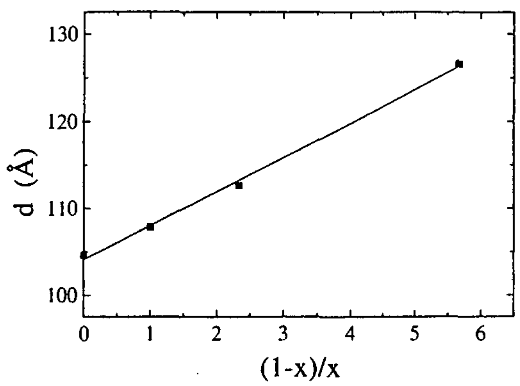

Figure 3. Variation of the *d*-layer spacing of polymers **Ia**–**d** as a function of the monomeric molar ratio at 150 °C.

the mesophase observed for these two copolymers was smectic A in nature.

The molecular organization of the mesomorphic units in the polymeric structure can be deduced by taking into account the above X-ray data and the structure of the ferrocene core. First, because of the bulkiness of the latter, the mesomorphic ferrocene units are, most likely, organized in an alternating way leading to a double layer (herringbone organization). Second, the ratio of the *d*-layer spacing obtained for polymer **Ia** (105 Å at 140 °C)[16] and the one of monomer **1c** (59.8 Å at 135 °C) within the smectic A phase gives a value of $d_{\mathrm{polymer}}/d_{\mathrm{monomer}} = 1.75$, suggesting an interdigitation of the layers and a disorganized state (folding, curling) of the flexible chains.

The influence of the monomeric ratio on the interlamellar distance was investigated by determining the *d*-layer spacing of **Ia**–**d** at 150 °C (Figure 3). Clearly, the layer thickness increased with the content of dimethylsiloxane units. This behavior was in agreement with literature data[17] obtained for other polysiloxanes and could be explained in terms of microphase separations: the amphipatic character between the different constituent parts of the polymer leads to a microsegregation in space of the polysiloxane backbone, the aromatic units, and the aliphatic chains, respectively. The overall layer thickness is the sum of the siloxane and mesogenic sublayers; since the smectic order is kept with dilution (i.e., there is no significant change in the lateral order of the side groups), it can be assumed that the increase of the smectic layer thickness corresponds mainly to the increase of the polysiloxane sublayer, as already reported for other types of liquid-crystalline polymers.[18] If such, the layer thickness should increase linearly as a function of $(1 - x)/x$, where x is the percentage of the ferrocene units. Thus, the slope of this linear variation can be estimated to be equal to V_{DMS}/S, where V_{DMS} is the volume of one dimethylsiloxane unit (ca. 145 Å^3 at 170 °C)[19] and S the molecular area of one mesogenic unit. The value found for this slope in the present work is about 4 Å and leads to an S value of about 36 Å^2. This value can be understood from the proposed stuctural model given in Figure 4. Indeed, due to the bulkiness of the ferrocene group (ca. 44 Å^2),[20] which is about twice that of the classical calamitic mesogenic part (ca. 23–26 Å^2), two successive side groups along the same side of the polymer backbone should be shifted along the normal to the smectic layers to fill the space efficiently. In such a description, the effective molecular area of each side group is about 33 Å^2 (see ref 21) a value which is compatible with the distance (6.2 Å) between the corresponding two silicon atoms along the polymer backbone. Finally, it is worth noting that such a molecular organization implies that the aliphatic chains (spacer and terminal chains) be highly disorganized and thus rather spread laterally, which is again in agreement with the values of the layer spacing observed (smaller than twice the molecular length of the monomer in the case of the homopolymer).

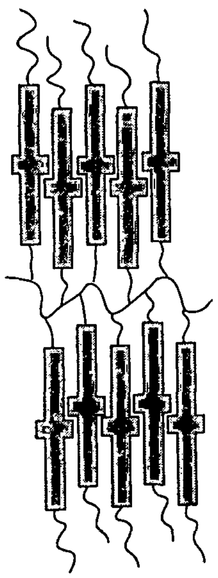

Figure 4. Proposed organization of the appended ferrocene units anchored onto the polymer within the smectic A phase.

Finally, the thermal stability of polymers **Ia**–**d** and **II** was examined by thermogravimetry. No decomposition was detected up to 250 °C, which indicated good thermal resistance of the investigated polymeric materials.

Conclusion

The above results and those obtained for ferrocene-containing thermotropic side-chain liquid-crystalline polymethacrylates[22] and thermotropic liquid-crystalline polyferrocenylsilanes[23] demonstrate that ferrocene is a valuable unit for designing ferrocene-based metallomesogenic polymers. Considering the numerous possibilities for functionalizing the ferrocene core,[5] the choice and positions of substituents may be used for tuning and controlling both the thermal and mesomorphic properties of such polymeric materials. Furthermore, our recent studies devoted to the design and study of chiral ferrocene-containing liquid crystals with planar chirality[9a] and ferrocenium-containing thermotropic liquid crystals[24] open the doors toward the development of new polymeric materials presenting interesting properties.

Experimental Section

Materials. CH_2Cl_2 (P_2O_5, under N_2) and toluene (sodium, benzophenone, under N_2) were distilled prior to use. Benzene (Fluka, puriss pa), benzyl alcohol (Fluka, puriss pa), pyridine (Fluka, puriss pa), oxalyl chloride (Fluka, purum), and triethylamine (Fluka, puriss pa) were used as received. Pyridine and triethylamine were stored on 4 Å molecular sieves. Compounds **3**[25] (from ferrocene-1,1′-dicarboxylic acid), **6** (n = 12, 18),[26] **10** (m = 6, 9),[27] and **11**[25,28] (from ferrocene) were synthesized by following literature procedures. Poly(hydrosiloxane)s **14a**–**d** [x = 1.0 (PS 120); x = 0.50–0.55 (PS 122.5); x = 0.30–0.35 (PS 123); x = 0.15–0.18 (PS 123.5)] were Hüls America Inc. products. Dichloro(1,5-cyclooctadiene)-

platinum(II) ($PtCl_2(1,5\text{-}C_8H_{12})$) was purchased from Strem Chemicals Inc. All reactions were carried out under N_2.

Techniques. Column chromatography used silica gel 60 (0.060−0.200 mm, SDS). Melting points (uncorrected) were determined on a Büchi 530 instrument. Transition temperatures (onset point for monomers; peak transition for polymers) and enthalpies were determined with a differential scanning Mettler DSC 30 calorimeter connected to a Mettler TA 4000 processor, under N_2, at a rate of 10 °C min^{-1} (for **1b**, 2 °C min^{-1}) (second heating run); Mettler TA72.2/0.5 GRAPHWARE was used for data treatment. Thermogravimetry analyses were performed with a Mettler TG 50 thermobalance connected to a Mettler TA 4000 processor at a rate of 10 °C min^{-1}. Optical studies were made using a Zeiss-Axioscop polarizing microscope equipped with a Linkam-THMS-600 variable-temperature stage, under N_2. Gel permeation chromatography (GPC) was made with a Waters 510 instrument connected to a Waters 410 differential refractometer. Ultrastyragel 10^3-10^4 columns were calibrated with polystyrene standards (eluent, THF, 1 mL min^{-1}; $T = 35$ °C; Baseline 510 software used for data treatment). ^1H NMR spectra were recorded in $CDCl_3$ on a Varian Gemini 200 spectrometer or a Bruker AMX 400 spectrometer, with the solvent as an internal standard. IR spectra were recorded on a Perkin-Elmer 1720 FTIR spectrometer. Elemental analyses were done by Mikroelementaranalytisches Laboratorium ETH-Zurich or Ciba (Marly, Switzerland).

X-ray Diffraction Studies. The crude powder was filled in Lindemann capillaries, and a linear monochromatic Cu Kα beam obtained with a sealed-tube generator and a bent quartz monochromator was used. The diffraction patterns were registered either with a curved proportional detector "Inel CPS 120" or photographically. In general, the position of the second-order reflection in the small-angle region was used to determine the layer spacing. The temperature was controlled within ±0.05 °C.

Synthesis. 1′-[(Benzyloxy)carbonyl]ferrocene-1-carboxylic acid (4). A solution of benzyl alcohol (3.71 g, 34.3 mmol) in CH_2Cl_2 (29 mL) was added dropwise to a stirred solution of **3** (10.6 g, 34.1 mmol) and triethylamine (6.89 g, 68.1 mmol) in CH_2Cl_2 (1430 mL); the addition was done in three times: 50% first, followed by twice 25% at 15 min intervals. The mixture was stirred at room temperature for a further 4 h and evaporated to dryness. Purification of the residue by column chromatograpy (first with 8:2 CH_2Cl_2/AcOEt to recover the diester and then with 8:2:0.1 CH_2Cl_2/AcOEt/AcOH) gave pure **4** (5.26 g, 42%). Mp = 154 °C. ^1H NMR (200 MHz): δ 7.50−7.34 (m, 5 H, aromatic protons, benzyl), 5.29 (s, 2 H, CH_2Ph), 4.91 (t, 2 H, HCp), 4.83 (t, 2 H, HCp), 4.47 (t, 2 H, HCp), 4.35 (t, 2 H, HCp).

1-(Chlorocarbonyl)-1′-[(benzyloxy)carbonyl]ferrocene (5). A solution of **4** (2.00 g, 5.50 mmol), oxalyl chloride (3.36 g, 26.5 mmol), and pyridine (20 drops) in CH_2Cl_2 (20 mL) was stirred under reflux for 7 h and evaporated to dryness. The solid residue was extracted with hot light petroleum until the extracts remained colorless. Evaporation of the solvent gave **5** (2.10 g, 100%), which was used in the next step without further purification. Mp = 70 °C. ^1H NMR (200 MHz): δ 7.50−7.38 (m, 5 H, aromatic protons, benzyl), 5.29 (s, 2 H, CH_2-Ph), 4.96 (t, 2 H, HCp), 4.87 (t, 2 H, HCp), 4.54 (t, 2 H, HCp), 4.48 (s, 2 H, HCp).

1-[(Benzyloxy)carbonyl]-1′-{*p*-{*p*′-[[(octadecyloxy)phenyl]oxy]carbonyl}[(phenyloxy)carbonyl]}ferrocene (7) (*n* = 18). A solution of **5** (2.10 g, 5.49 mmol), **6** (n = 18) (2.65 g, 5.49 mmol), and triethylamine (0.53 g, 5.2 mmol) in CH_2Cl_2 (40 mL) was heated under reflux overnight and evaporated to dryness. Purification of the residue by column chromatography (50:1 CH_2Cl_2/AcOEt) and crystallization (CH_2Cl_2/EtOH) gave pure **7** (n = 18) (4.0 g, 88%). Mp = 91−92 °C. ^1H NMR (400 MHz): δ 8.23 (d, 2 H, aromatic protons), 7.42−7.33 (m, 7 H, aromatic protons), 7.13 (d, 2 H, aromatic protons), 6.94 (d, 2 H, aromatic protons), 5.25 (s, 2 H, CH_2Ph), 4.95 (t, 2 H, HCp), 4.91 (t, 2 H, HCp), 4.52 (t, 2 H, HCp), 4.44 (t, 2 H, HCp), 3.97 (t, 2 H, CH_2O), 1.79 (m, 2 H, CH_2CH_2O), 1.46 (m, 2 H, $CH_2CH_2CH_2O$), 1.26 (m, 28 H, aliphatic protons), 0.88 (t, 3 H, CH_3). Anal. Calcd for $C_{50}H_{60}O_7Fe$ (828.87): C, 72.45; H, 7.30. Found: C, 72.48; H, 7.35.

Compound **7** (n = 12) was prepared from **6** (n = 12) by following the above synthetic procedure and gave analytical data which were in agreement with its structure.

1′-{*p*-{*p*′-[[(octadecyloxy)phenyl]oxy]carbonyl}[(phenyloxy)carbonyl]}ferrocene-1-carboxylic acid (8) (*n* = 18). A mixture of **7** (n = 18) (6.04 g, 7.29 mmol), Pd (10%)/C (0.6 g) and 2:3 CH_2Cl_2/EtOH (500 mL) was stirred overnight at room temperature under 4 bar of H_2. The mixture was filtered and the solvent evaporated to dryness. Purification of the residue by crystallization (EtOH) gave pure **8** (n = 18) (4.71 g, 87%). Mp = 176−178 °C. ^1H NMR (400 MHz): δ 8.27 (d, 2 H, aromatic protons), 7.39 (d, 2 H, aromatic protons), 7.12 (d, 2 H, aromatic protons), 6.93 (d, 2 H, aromatic protons), 5.01 (s, 2 H, HCp), 4.95 (s, 2 H, HCp), 4.57 (d, 4 H, HCp), 3.96 (t, 2 H, CH_2O), 1.78 (m, 2 H, CH_2CH_2O), 1.46 (m, 2 H, $CH_2CH_2CH_2O$), 1.26 (m, 28 H, aliphatic protons), 0.88 (t, 3 H, CH_3). Anal. Calcd for $C_{43}H_{54}O_7Fe$ (738.74): C, 69.91; H, 7.37. Found: C, 69.89; H, 7.32.

Compound **8** (n = 12) was prepared from **7** (n = 12) by following the above synthetic procedure and gave analytical data which were in agreement with its structure.

1-(Chlorocarbonyl)-1′-{*p*-{*p*′-[[(octadecyloxy)phenyl]oxy]carbonyl}[(phenyloxy)carbonyl]}ferrocene (9) (*n* = 18). A solution of **8** (n = 18) (1.57 g, 2.13 mmol), oxalyl chloride (1.40 g, 11.0 mmol), and pyridine (6 drops) in CH_2Cl_2 (90 mL) was heated under reflux for 7 h and evaporated to dryness. The solid residue was extracted with hot light petroleum until the extracts remained colorless. Evaporation of the solvent gave **9** (n = 18) (1.41 g, 87%), which was used in the next step without further purification. Mp = 103−105 °C. ^1H NMR (400 MHz): δ 8.27 (d, 2 H, aromatic protons), 7.38 (d, 2 H, aromatic protons), 7.12 (d, 2 H, aromatic protons), 6.93 (d, 2 H, aromatic protons), 5.10 (t, 2 H, HCp), 5.03 (t, 2 H, HCp), 4.74 (t, 2 H, HCp), 4.68 (t, 2 H, HCp), 3.96 (t, 2 H, CH_2O), 1.79 (m, 2 H, CH_2CH_2O), 1.47 (m, 2 H, $CH_2CH_2CH_2O$), 1.26 (m, 28 H, aliphatic protons), 0.88 (t, 3 H, CH_3).

Compound **9** (n = 12) was prepared from **8** (n = 12) by following the above synthetic procedure and gave analytical data which were in agreement with its structure.

1-{*p*-{*p*′-[[(Undec-10-enyloxy)benzoyl]oxy]}[(phenyloxy)carbonyl]}-1′-{*p*-{*p*′-[[(octadecyloxy)phenyl]oxy]carbonyl}[(phenyloxy)carbonyl]}ferrocene (1c). A solution of **9** (n = 18) (1.02 g, 1.35 mmol), **10** (m = 9) (0.57 g, 1.49 mmol), and triethylamine (0.14 g, 1.38 mmol) in CH_2Cl_2 (35 mL) was heated under reflux overnight and evaporated to dryness. Purification of the residue by column chromatography (100:1 CH_2Cl_2/AcOEt) and crystallization (CH_2Cl_2/EtOH) gave pure **1c** (1.04 g, 70%). ^1H NMR (400 MHz): δ 8.22 (d, 2 H, aromatic protons), 8.12 (d, 2 H, aromatic protons), 7.34 (d, 2 H, aromatic protons), 7.22 (d, 4 H, aromatic protons), 7.11 (d, 2 H, aromatic protons), 6.96 (d, 2 H, aromatic protons), 6.91 (d, 2 H, aromatic protons), 5.82 (m, 1 H, $CH{=}CH_2$), 5.09 (m, 4 H, HCp), 5.03−4.92 (m, 2 H, $CH{=}CH_2$), 4.64 (m, 4 H, HCp), 4.04 (t, 2 H, CH_2O), 3.95 (t, 2 H, CH_2O), 2.06 (m, 2 H, $CH_2CH{=}CH_2$), 1.80 (m, 4 H, CH_2CH_2O), 1.46 (m, 4 H, $CH_2CH_2CH_2O$), 1.41−1.26 (m, 38 H, aliphatic protons), 0.88 (t, 3 H, CH_3). IR (KBr): 3126, 3077, 2920, 2850, 1739, 1722, 1642, 1606, 1510, 1471, 1454 cm^{-1}. Anal. Calcd for $C_{67}H_{82}O_{10}Fe$ (1103.23): C, 72.94; H, 7.49. Found: C, 72.96; H, 7.55.

Monomers **1a** [from **9** (n = 12) and **10** (m = 6)] and **1b** [from **9** (n = 18) and **10** (m = 6)] were prepared by following the above synthetic procedure and gave analytical data which were in agreement with their structures.

3-{*p*-{*p*′-[[(Octadecyloxy)phenyl]oxy]carbonyl}[(phenyloxy)carbonyl]}ferrocene-1-carboxylic acid (12). A solution of **11** (0.31 g, 1.0 mmol), **6** (n = 18) (0.48 g, 1.0 mmol), and pyridine (a few drops) in benzene (70 mL) was heated under reflux for 36 h and evaporated to dryness. Purification of the residue by column chromatography (first with CH_2Cl_2, then with 10:1 CH_2Cl_2/AcOEt, and finally with 10:1:0.1 CH_2Cl_2/AcOEt/AcOH) and crystallization (CH_2Cl_2/hexane) gave pure **12** (0.19 g, 26%). Mp = 180 °C. ^1H NMR

(400 MHz): δ 8.29 (d, 2 H, aromatic protons), 7.33 (d, 2 H, aromatic protons), 7.12 (d, 2 H, aromatic protons), 6.94 (d, 2 H, aromatic protons), 5.73 (s, 1 H, HCp), 5.34 (s, 1 H, HCp), 5.20 (s, 1 H, HCp), 4.49 (s, 5 H, HCp), 3.97 (t, 2 H, CH_2O), 1.79 (m, 2 H, CH_2CH_2O), 1.46 (m, 2 H, $CH_2CH_2CH_2O$), 1.26 (m, 28 H, aliphatic protons), 0.88 (t, 3 H, CH_3). Anal. Calcd for $C_{43}H_{54}O_7Fe$ (738.74): C, 69.91; H, 7.37. Found: C, 70.05; H, 7.22.

1-(Chlorocarbonyl-3-{*p*-{*p*′-[[(octadecyloxy)phenyl]oxy]carbonyl}[(phenyloxy)carbonyl]}ferrocene (13). A solution of **12** (0.45 g, 0.61 mmol), oxalyl chloride (0.38 g, 3.0 mmol), and pyridine (5 drops) in CH_2Cl_2 (15 mL) was heated under reflux for 7 h and evaporated to dyness. The solid residue was extracted with hot light petroleum until the extracts remained colorless. Evaporation of the solvent gave **13** (0.39 g, 84%), which was used in the next step without further purification. Mp = 120–125 °C. ^1H NMR (200 MHz): δ 8.29 (d, 2 H, aromatic protons), 7.33 (d, 2 H, aromatic protons), 7.13 (d, 2 H, aromatic protons), 6.94 (d, 2 H, aromatic protons), 5.74 (t, 1 H, HCp), 5.35 (m, 1 H, HCp), 5.21 (m, 1 H, HCp), 4.50 (s, 5 H, HCp), 3.97 (t, 2 H, CH_2O), 1.79 (m, 2 H, CH_2CH_2O), 1.26 (m, 30 H, aliphatic protons), 0.88 (t, 3 H, CH_3).

1-{*p*-{*p*′-[[(Undec-10-enyloxy)benzoyl]oxy]}[(phenyloxy)carbonyl]}-3-{*p*-{*p*′-[[(octadecyloxy)phenyl]oxy]carbonyl}[(phenyloxy)carbonyl]}ferrocene (2). A solution of **13** (0.12 g, 0.16 mmol), **10** ($m = 9$) (0.080 g, 0.21 mmol), and triethylamine (16 mg, 0.16 mmol) in CH_2Cl_2 (15 mL) was heated under reflux overnight and evaporated to dryness. Purification of the residue by column chromatography (100:1 CH_2Cl_2/AcOEt) and crystallization (CH_2Cl_2/EtOH) gave pure **2** (0.11 g, 62%). ^1H NMR (400 MHz): δ 8.29 (d, 2 H, aromatic protons), 8.15 (d, 2 H, aromatic protons), 7.35 (d, 2 H, aromatic protons), 7.29 (d, 2 H, aromatic protons), 7.26 (d, 2 H, aromatic protons), 7.13 (d, 2 H, aromatic protons), 6.98 (d, 2 H, aromatic protons), 6.94 (d, 2 H, aromatic protons), 5.79 (t, 1 H, HCp), 5.83–5.78 (m, 1 H, $CH{=}CH_2$), 5.28–5.25 (m, 2 H, HCp), 5.02–4.92 (m, 2 H, $CH{=}CH_2$), 4.47 (s, 5 H, HCp), 4.05 (t, 2 H, CH_2O), 3.97 (t, 2 H, CH_2O), 2.05 (m, 2 H, $CH_2CH{=}CH_2$), 1.81 (m, 4 H, CH_2CH_2O), 1.46 (m, 4 H, $CH_2CH_2CH_2O$), 1.41–1.26 (m, 38 H, aliphatic protons), 0.88 (t, 3 H, CH_3). IR (KBr): 3131, 3079, 2920, 2851, 1733, 1722, 1641, 1606, 1510, 1466 cm^{-1}. Anal. Calcd for $C_{67}H_{82}O_{10}Fe$ (1103.23): C, 72.94; H, 7.49. Found: C, 72.98; H, 7.20.

Synthesis of Polymer Ia. A solution of poly(methylhydroxysiloxane) **14a** (0.024 g, 0.41 mmol of SiH units) in toluene (5 mL) was added to a solution of monomer **1c** (0.5 g, 0.45 mmol) in toluene (13 mL). The mixture was heated to 70 °C, and $PtCl_2(1,5\text{-}C_8H_{12})$ (0.9 mg, 2.4×10^{-3} mmol) was then added. The solution was heated at 70 °C for 24 h and evaporated to dryness. Purification of the residue by dissolution in CH_2Cl_2 and precipitation with MeOH gave **Ia** (0.15 g, 32%). The purification process was repeated until no monomer was detected by GPC. ^1H NMR (400 MHz): δ 8.21 (br s, 2 H, aromatic protons), 8.10 (br s, 2 H, aromatic protons), 7.31 (br d, 2 H, aromatic protons), 7.21 (br s, 2 H, aromatic protons), 7.09 (br s, 2 H, aromatic protons), 6.90 (br d, 4 H, aromatic protons), 5.08 (br s, 4 H, HCp), 4.63 (br s, 4 H, HCp), 4.01 (br s, 2 H, CH_2O), 3.94 (br s, 2 H, CH_2O), 1.78 (br s, 4 H, CH_2CH_2O), 1.45 (br s, 4 H, $CH_2CH_2CH_2O$), 1.25 (br m, 38 H, aliphatic protons), 0.86 (br s, 3 H, CH_3), 0.51 (br s, 2 H, CH_2Si), 0.08 (br m, 123 H, CH_3Si). IR (KBr): 3126, 3078, 2921, 2851, 1738, 1606, 1580, 1510, 1456 cm^{-1}.

Polymers **Ib** (from **14b**), **Ic** (from **14c**), **Id** (from **14d**), and **II** (from **2** and **14d**) were prepared by following the above synthetic procedure and gave analytical data which were in agreement with their structures.

Acknowledgment. R.D. acknowledges the Swiss National Science Foundation (Grant No. 20-45588.95) for financial support, the Doktoranden-Stipendien der Chemischen Industrie, Basel, for a fellowship to I.J, and Pluto/Veba Oel, Germany, for a generous gift of the ferrocene-1,1′-dicarboxylic acid.

References and Notes

(1) White, M. S. In *Siloxane Polymers*; Clarson, S. J., Semlyen, J. A., Eds.; PTR Prentice Hall, Inc.: Englewood Cliffs, NJ, 1993; Chapter 6.

(2) Dumon, M.; Zentel, R.; Kulinnas, C.; Siesler, H. W. *Liq. Cryst.* **1995**, *18*, 903.

(3) (a) Abe, J.; Hasegawa, M.; Matsushima, H.; Shirai, Y.; Nemoto, N.; Nagase, Y.; Takamiya, N. *Macromolecules* **1995**, *28*, 2938. (b) Wischerhoff, E.; Zentel, R.; Fischer, H. *J. Chem. Soc., Faraday Trans.* **1994**, *90*, 3331.

(4) (a) *Metallomesogens: Synthesis, Properties and Applications;* Serrano, J. L., Ed.; VCH: Weinheim, Germany, 1996. (b) Bruce, D. W. In *Inorganic Materials*, 2nd ed.; Bruce, D. W., O'Hare, D., Eds.; Wiley: Chichester, U.K., 1996; Chapter 8. (c) Bruce, D. W. *J. Chem. Soc., Dalton Trans.* **1993**, 2983. (d) Hudson, S. A.; Maitlis, P. M. *Chem. Rev.* **1993**, *93*, 861. (e) Espinet, P.; Esteruelas, M. A.; Oro, L. A.; Serrano, J. L.; Sola, E. *Coord. Chem. Rev.* **1992**, *117*, 215. (f) Giroud-Godquin, A.-M.; Maitlis, P. M. *Angew. Chem., Int. Ed. Engl.* **1991**, *30*, 375.

(5) For ferrocene-containing thermotropic liquid crystals, see the following review: Deschenaux, R.; Goodby, J. W. In *Ferrocenes: Homogeneous Catalysis, Organic Synthesis, Materials Science*; Togni, A., Hayashi, T., Eds.; VCH: Weinheim, Germany, 1995; Chapter 9.

(6) Ruthenocene-containing thermotropic liquid crystals: Deschenaux, R.; Santiago, J. *J. Mater. Chem.* **1993**, *3*, 219.

(7) Mesomorphic (η^6-arene)tricarbonylchromium complexes: Campillos, E.; Deschenaux, R.; Levelut, A.-M.; Ziessel, R. *J. Chem. Soc., Dalton Trans.* **1996**, 2533.

(8) (a) Oriol, L.; Pinol, M.; Serrano, J. L. *Prog. Polym. Sci.* **1997**, *22*, 873. (b) Oriol, L. In ref 4a, chapter 5. (c) Oriol, L.; Serrano, J. L. *Adv. Mater.* **1995**, *7*, 348.

(9) (a) Deschenaux, R.; Santiago, J. *Tetrahedron Lett.* **1994**, *35*, 2169. (b) Deschenaux, R.; Rama, M.; Santiago, J. *Tetrahedron Lett.* **1993**, *34*, 3293.

(10) Deschenaux, R.; Kosztics, I.; Scholten, U.; Guillon, D.; Ibn-Elhaj, M. *J. Mater. Chem.* **1994**, *4*, 1351.

(11) Gray, G. W.; Lacey, D.; Nestor, G.; White, M. S. *Makromol. Chem., Rapid Commun.* **1986**, *7*, 71.

(12) Two values are given for copolymers **Ib–d** and **II**: the minimum value was calculated from the lower molecular weight (as indicated by the supplier) and CH_3SiH monomeric content, whereas the maximum value was calculated from the higher molecular weight (as indicated by the supplier) and CH_3SiH monomeric content. Example: for **Ib**, the values $x = 0.50$ with a PM = 900 and $x = 0.55$ with a PM = 1000 were used to calculate the minimum and maximum molecular weight, respectively.

(13) Deschenaux, R.; Kosztics, I.; Marendaz, J.-L.; Stoeckli-Evans, H. *Chimia* **1993**, *47*, 206.

(14) Khan, M. A.; Bhatt, J. C.; Fung, B. M.; Nicholas, K. M.; Wachtel, E. *Liq. Cryst.* **1989**, *5*, 285.

(15) Deschenaux, R.; Santiago, J.; Guillon, D.; Heinrich, B. *J. Mater. Chem.* **1994**, *4*, 679.

(16) Note that the *d*-values reported in this paper correspond to about twice those reported in our preliminary communication.[10] We have used here a small-angle X-ray diffraction camera well suited to observe large polymer periodicity (a few hundred Å), while, in our preliminary report,[10] the X-ray diffraction signals corresponding to the first Bragg reflection were masked by the beam stop.

(17) Poths, H.; Zentel, R. *Liq. Cryst.* **1994**, *16*, 749.

(18) Navarro-Rodriguez, D.; Guillon, D.; Skoulios, A.; Frère, Y.; Gramain, Ph. *Makromol. Chem.* **1992**, *193*, 3117.

(19) Katoaka, T.; Ueda, S. *Polym. Lett.* **1966**, *4*, 317.

(20) This value was estimated by high-resolution dilatometric measurements for dioctylferrocene at 50 °C: (690 Å^3 − 500 Å^3)/4.3 Å ≈ 44 Å^2, where 690 Å^3 is the total molecular volume of dioctylferrocene, 500 Å^3 is the molecular volume of the two alkyl chains, and 4.3 Å is the length of the Cp ring. The value of 500 Å^3 was obtained from: Doolittle, A. K. *J. Appl. Phys.* **1951**, *22*, 1471. The 44 Å^2 value was confirmed from crystallographic data (Seiler, P.; Dunitz, J. D. *Acta Crystallogr.* **1979**, *35B*, 2020. McDonald, A. C.; Trotter, J. *Acta Crystallogr.* **1964**, *17*, 872).

(21) The effective molecular area was calculated as follows: [44 + 44/2]/2 ≈ 33 Å^2, where 44 Å^2 represents the estimated molecular area of the ferrocene unit.[20]

(22) (a) Deschenaux, R.; Turpin, F.; Guillon, D. *Macromolecules* **1997**, *30*, 3759. (b) Deschenaux, R.; Izvolenski, V.; Turpin, F.; Guillon, D.; Heinrich, B. *Chem. Commun.* **1996**, 439.

(23) (a) Liu, X.-H.; Bruce, D. W.; Manners, I. *J. Organomet. Chem.* **1997,** *548*, 49. (b) Liu, X.-H.; Bruce, D. W.; Manners, I. *Chem. Commun.* **1997,** 289.

(24) Deschenaux, R.; Schweissguth, M.; Levelut, A.-M. *Chem. Commun* **1996,** 1275.

(25) Knobloch, F. W.; Rauscher, W. H. *J. Polym. Sci.* **1961,** *54*, 651.

(26) Deschenaux, R.; Marendaz, J.-L.; Santiago, J. *Helv. Chim. Acta* **1994,** *76*, 865.

(27) (a) Dumon, M.; Nguyen, H. T.; Mauzac, M.; Destrade, C.; Gasparoux, H. *Liq. Cryst.* **1991,** *10*, 475. (b) Kelly, S. M.; Buchecker, R. *Helv. Chim. Acta* **1988,** *76*, 865.

(28) (a) Hisatome, M.; Tachikawa, O.; Sasho, M.; Yamakawa, K. *J. Organomet. Chem.* **1981,** *217*, C17. (b) Kasahara, A.; Izumi, T.; Yoshida, Y.; Shimizu, I. *Bull. Chem. Soc. Jpn* **1981,** *55*, 1901. (c) Nesmeyanov, A. N.; Leonova, E. V.; Kochetkova, N. S.; Malkova, A. I.; Makarovskaya, A. G. *J. Organomet. Chem.* **1975,** *96*, 275.

MA980410W

Columnar Phases from Covalent and Hydrogen-Bonded Liquid-Crystalline Ferrocene Derivatives

Preliminary Communication

by **Robert Deschenaux***, **Florence Monnet**, **Elisabeth Serrano**, and **François Turpin**

Institut de Chimie, Université de Neuchâtel, Av. de Bellevaux 51, CH-2000 Neuchâtel

and **Anne-Marie Levelut***

Université Paris-Sud, Laboratoire de Physique des Solides, Bâtiment 510, F-91405 Orsay Cedex

The synthesis and liquid-crystalline properties of tetracatenar covalent and H-bonded bis-ferrocene derivatives **1** and **2**, respectively, are reported. Both compounds gave rise to enantiotropic columnar liquid-crystalline behavior with a hexagonal molecular organization. To explore the possibility to obtain also calamitic liquid-crystalline phases from H-bonded ferrocene-containing liquid crystals, a rod-shaped ferrocene mesogen **3** was synthesized, which gave rise to enantiotropic smectic C and smectic A phases. For the first time, a rational synthetic design at the ferrocene level led to ferrocene-based liquid-crystals with columnar behavior and to H-bonded metallomesogens.

Introduction. – Current efforts oriented towards the development of ferrocene-based mesomorphic materials led to the synthesis of ferrocene-containing side-chain liquid-crystalline polymers [1], ferrocene-containing liquid-crystalline dendrimers [2], and a liquid-crystalline mixed [60]fullerene-ferrocene derivative [3]. These structures are promising candidates to construct switchable anisotropic materials. We demonstrated that electron transfer can be used to generate mesomorphism in the ferrocene-ferrocenium redox system [4].

To further explore the *structure/supramolecular organization* relationship in the case of ferrocene-containing mesomorphic molecular units, the study of novel structures is required. Mesomorphic ferrocenes exhibiting columnar liquid-crystalline phases would be of particular interest: No such examples have been reported [5–7]¹). Because of the bulky, three-dimensional structure of the ferrocene core, the primary influence of which is to reduce the intermolecular interactions (resulting in a lowering of the liquid-crystalline tendency in comparison with the ferrocene-free analogues) [5], the design of such compounds represents both a conceptual and synthetic challenge. Ultimately, owing to its redox activity, the incorporation of ferrocene units into columnar phases may open the doors to new supramolecular wires [9].

---

¹) A liquid-crystalline ferrocenyl-phthalocyanine derivative (the ferrocene unit is located at the end of one alkyl chain) showing a discotic phase was described [8]; even if the discotic phase was induced by the phthalocyanine core, this example is important as it shows that ferrocene can accomodate to discotic phases.

We report, herein, the synthesis and liquid-crystalline properties of the tetracatenar ferrocene derivatives **1** and **2**. A tetracatenar system was selected to design ferrocene derivatives showing columnar phases in view of successful investigations made for organic liquid crystals [10]. Furthermore, to explore the possibility to use H-bonds to design ferrocene-containing thermotropic liquid crystals exhibiting calamitic liquid-crystalline phases, the rod-like-shaped H-bonded ferrocene complex **3** was synthesized. Compounds **2** and **3** represent the first H-bonded metallomesogens described so far [5–7]. Note that the H-bonds were elegantly used to elaborate ferrocene-based sensors [11].

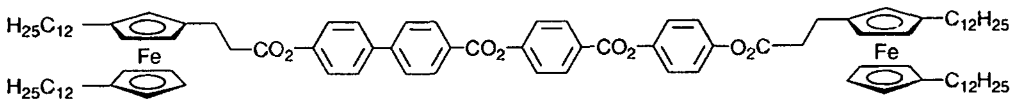

1

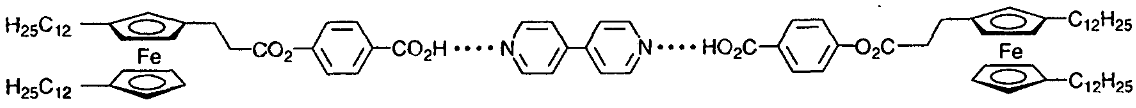

2

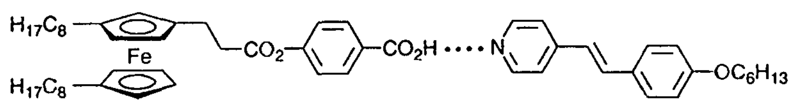

3

Results and Discussion. – The syntheses of **1**–**3** are illustrated in *Schemes 1–3*, respectively[2]. The preparation of **1** (and of the ferrocene intermediates) required an esterification-deprotection sequence. The H-bonded complexes **2** and **3** were prepared by reacting the appropriate acid and pyridine derivatives in THF at room temperature. The formation of H-bonds was confirmed by FT-IR spectroscopy [13]. The structure and purity of all compounds were confirmed by NMR spectroscopy and elemental analysis.

The liquid-crystalline properties of **1** and **2** were examined by a combination of differential scanning calorimetry (DSC), polarized optical microscopy (POM), and

---

[2] Ferrocene derivatives **4** and **5** were prepared analogously to their dioctyl homologues [1a]. Compounds **6** [1a] and **7** [12] were synthesized as published. Benzyl 4'-hydroxy-[1,1'-biphenyl]-4-carboxylate (*Step a* in *Scheme 1*) was obtained from 4'-hydroxy-[1,1'-biphenyl]-4-carboxylic acid and benzyl bromide (MeCN, 1,8-diazabicyclo[5.4.0]undec-7-ene (DBU), 70°, 5 h; yield 78%; purification by column chromatography; (silica gel, CH_2Cl_2) and crystallization from acetone/hexane). Benzyl 4-hydroxybenzoate (*Fluka*, ≥98%), 4,4'-bipyridyl (*Fluka*, ≥99%), and 4'-hydroxy-[1,1'-biphenyl]-4-carboxylic acid (*Aldrich*, 99%) were used as received.

Scheme 1

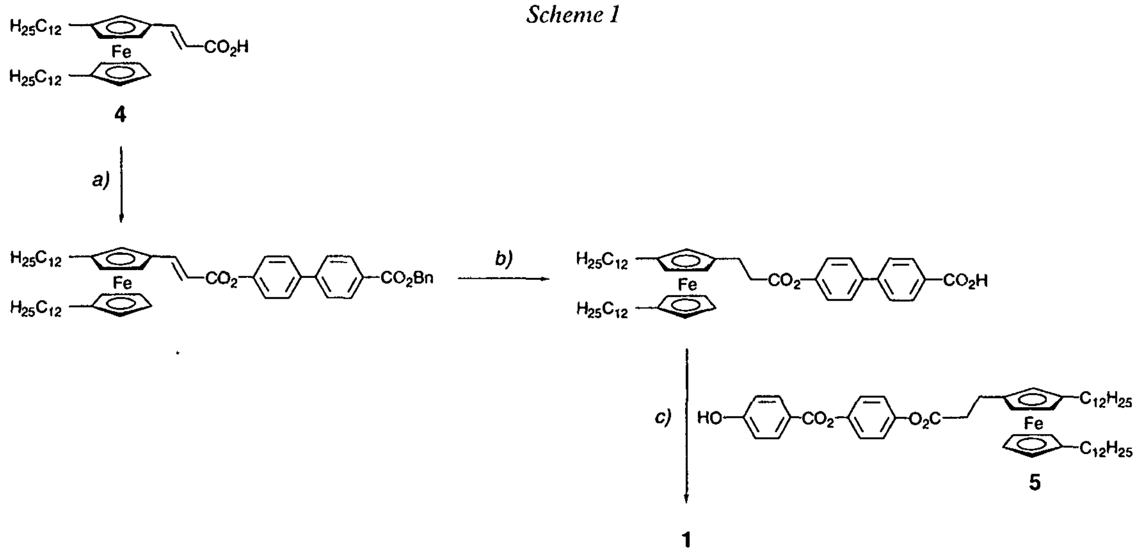

a) Benzyl 4'-hydroxy-[1,1'-biphenyl]-4-carboxylate, *N*,*N*'-dicyclohexylcarbodiimide (DCC), 4-(pyrrolidin-1-yl)pyridine (4-ppy), CH_2Cl_2, r.t., 3 h; 74%; purification by column chromatography (CC; silica gel, CH_2Cl_2). *b*) H_2, 10% Pd/C, CH_2Cl_2, r.t., 16 h; 90%; purification by CC (silica gel, Et_2O). *c*) DCC, 4-ppy, CH_2Cl_2, r.t., 3 h; 89%; purification by CC (silica gel, CH_2Cl_2).

Scheme 2

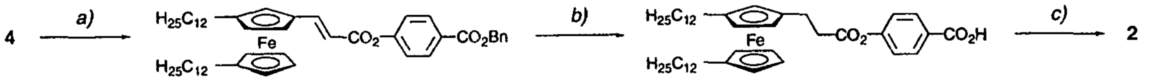

a) Benzyl 4-hydroxybenzoate, DCC, 4-(dimethylamino)pyridine (DMAP), CH_2Cl_2, r.t., overnight; 87%; purification by CC (silica gel, CH_2Cl_2). *b*) H_2, 10% Pd/C, CH_2Cl_2, r.t., 1 h; 73%; purification by dissolution in hexane and precipitation in MeOH. *c*) 4,4'-Bipyridine, THF, r.t., 0.5 h; 80%; purification by trituration with hexane, filtration, and washing with hexane.

X-ray diffraction (XRD)[3]. The mesomorphic behavior of **3** was investigated by DSC and POM. The thermal and liquid-crystalline data of **1**–**3** are reported in *Table 1*.

Both compounds **1** and **2** gave rise to birefringent fluids as detected by POM. Slow cooling of **1** from the isotropic fluid revealed the formation of spherulites and linear birefringent defects; a similar texture was observed for **2**. From these observations, the mesophases displayed by **1** and **2** were identified as columnar phases.

Compound **3** showed enantiotropic smectic C and smectic A phases which were identified from their textures: The smectic C phase gave rise to focal-conic and *schlieren* textures; as for the smectic A phase, a focal-conic texture and homeotropic areas were observed. The mesomorphic behavior of **3** is similar to that observed for an analogous covalent ferrocene derivative [1a].

The XRD confirmed the columnar nature of the liquid-crystalline phases of **1** and **2**. In both cases, a broad diffuse halo was observed for a scattering angle of 20°. This diffuse halo characterized the molten state of the alkyl chains and the lateral

---

[3] Instrumentation and techniques, see [14]. X-Ray diffraction experiments were performed using a monochromatic CuK_α beam with a section of *ca.* 0.25 mm^2. The sample temperature was maintained within ±0.2 K. The imaging-plate detector was read out by a molecular-dynamic system, and the detector to sample distance varied between 65 and 300 mm.

Scheme 3

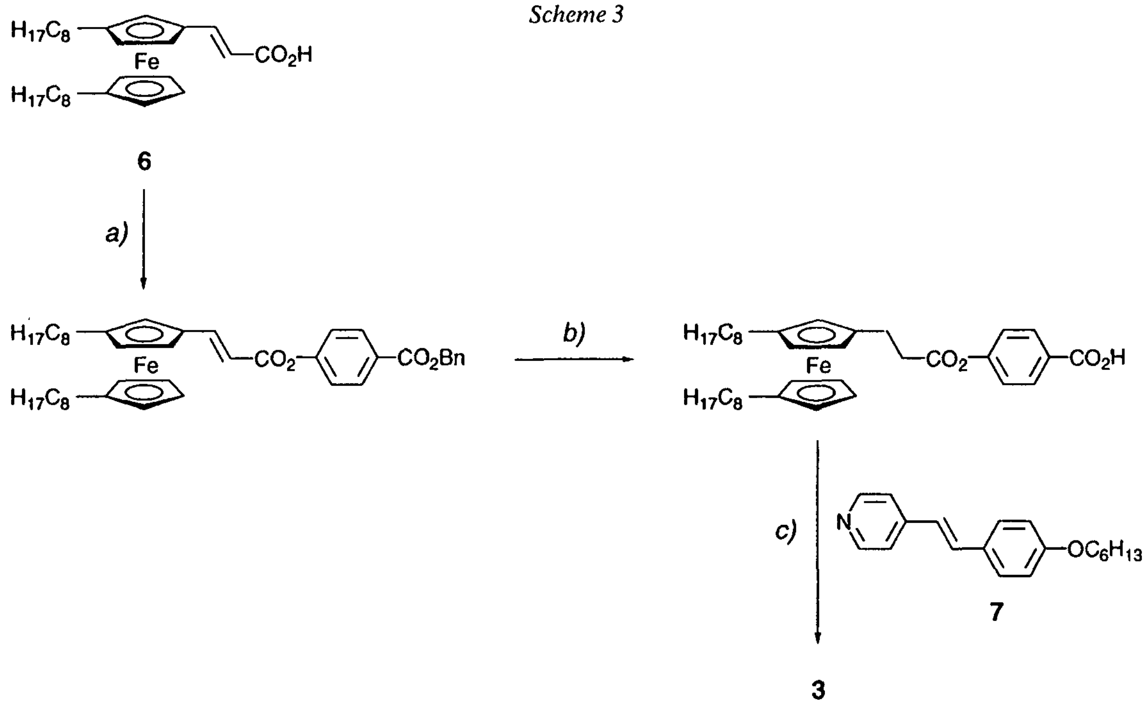

a) Benzyl 4-hydroxybenzoate, DCC, 4-ppy, CH_2Cl_2, r.t., overnight, 95%; purification by CC (silica gel, CH_2Cl_2). *b*) H_2, 10% Pd/C, CH_2Cl_2, r.t., 2 h; 89%; purification by CC (silica gel, CH_2Cl_2/MeOH 99:1). *c*) THF, r.t., 0.5 h; 80%; purification by trituration with hexane, filtration, and washing with hexane.

Table 1. *Phase Transitions and Enthalpy Changes of Compounds* **1**–**3**

	Phase transition[a])	T [°C][b])	ΔH [kJ mol^{-1}]
1	K → Col_h	52	65
	Col_h → I	84	2.8
2	K → Col_h	66	91
	Col_h → I	72	3.0
3	K → S_C	55	64
	S_C → S_A[c])	84	–
	S_A → I	101	7.9

[a]) K, crystalline state; Col_h, hexagonal columnar phase; S_C, smectic C phase; S_A, smectic A phase; I, isotropic liquid. [b]) Onset transition determined during the first heating run (10° min^{-1}, under N_2). [c]) Determined by polarized optical microscopy.

organization of the rod-like cores. For compound **1**, three sharp rings were seen at low angles corresponding to lattice spacings in $1:\sqrt{3}:2$ ratios. These three sharp rings revealed a hexagonal organization with a lattice constant $a = 49.8$ Å (*Table 2*). The structure of compound **2** is very similar to the one of **1**, but the mesophase growed in large domains so that the innermost ring was made of less than ten dinstinct spots. At larger angles, one could see spots corresponding to the 110 or 200 positions of a hexagonal lattice. However, only two or three spots of weak intensity were seen for each kind. Interestingly, both compounds **1** and **2** gave exactly the same lattice constant (*Table 2*).

Table 2. Bragg *Reflections, Lattice Constant* a [Å] *and Observed and Calculated* d *Spacings* [Å]

			Compound **1**			Compound **2**		
h	k	l	a	d_{obs}[a])	d_{calc}	a	d_{obs}[a])	d_{calc}
1	0	0	49.8	43.2	43.1	49.8	42.9	42.9
1	1	0		25.0	24.9		24.8	24.8
2	0	0		21.4	21.5		21.5	21.5

[a]) Recorded at 60°.

As for phasmidic compounds [15], the organization of the molecules in a column was more like that of lyotropic molecules in a cylinder, rather than like that of disc-like molecules stacked one above the other. There were five to six molecules in a slice of column 4.5 Å thick. Finally, the large lattice constant was in agreement with the length of the rigid core.

Conclusion. – The results presented in this report are of interest for three reasons. Firstly, ferrocene-containing thermotropic liquid crystals showing columnar phases are obtained. This finding, associated with data we already described [1–5], establishes that structural engineering at the ferrocene level can be exploited for tuning the molecular organization of ferrocene-based mesomorphic molecular units within the liquid-crystalline state. Secondly, the elaboration of metallomesogens through H-bonds opens unique opportunities for exploiting the properties of metals in novel supramolecular liquid-crystalline materials [16]. Finally, oxidation of one ferrocene unit in **1** or **2** will lead to mixed ferrocene-ferrocenium metallomesogens which will be sensitive to both oxidation and reduction processes. New properties and behavior are expected from such systems.

R.D. acknowledges the *Swiss National Science Foundation* for financial support (grants no. 20-45588.95 and 20-52295.97).

REFERENCES

[1] a) R. Deschenaux, F. Turpin, D. Guillon, *Macromolecules* **1997**, *30*, 3759; b) R. Deschenaux, V. Izvolenski, F. Turpin, D. Guillon, B. Heinrich, *Chem. Commun.* **1996**. 439; c) R. Deschenaux, I. Kosztics, U. Scholten, D. Guillon, M. Ibn-Elhaj, *J. Mater. Chem.* **1994**, *4*, 1351; d) R. Deschenaux, I. Jauslin, U. Scholten, F. Turpin, D. Guillon, B. Heinrich, *Macromolecules* **1998**. *31*, 5647.

[2] R. Deschenaux, E. Serrano, A.-M. Levelut, *Chem. Commun.* **1997**, 1577.

[3] R. Deschenaux, M. Even, D. Guillon, *Chem. Commun.* **1998**, 537.

[4] R. Deschenaux, M. Schweissguth, A.-M. Levelut, *Chem. Commun.* **1996**, 1275.

[5] R. Deschenaux, J. W. Goodby, in 'Ferrocenes: Homogeneous Catalysis, Organic Synthesis, Materials Science', Eds. A. Togni and T. Hayashi, VCH, Weinheim. 1995, Chapt. 9.

[6] D. W. Bruce, in 'Inorganic Materials', 2nd edn., Eds. D. W. Bruce and D. O'Hare, Wiley, Chichester, 1996, Chapt. 8.

[7] 'Metallomesogens: Synthesis, Properties, and Applications', Ed. J. L. Serrano, VCH, Weinheim, 1996.

[8] M. J. Cook, G. Cooke, A. Jafari-Fini, *Chem. Commun.* **1995**, 1715.

[9] C. F. van Nostrum, *Adv. Mater.* **1996**, *8*, 1027; C. F. van Nostrum, R. J. M. Nolte, *J. Chem. Soc., Chem. Commun.* **1996**, 2385.

[10] H.-T. Nguyen, C. Destrade, J. Malthête, *Adv. Mater*, **1997**, *9*, 375.

[11] J. D. Carr, L. Lambert, D. E. Hibbs, M. B. Hursthouse, K. M. Abdul Malik, J. H. R. Tucker, *Chem. Commun.* **1997**, 1649.

[12] D. W. Bruce, D. A. Dunmur, E. Lalinde, P. M. Maitlis, P. Styring, *Liq. Cryst.* **1988**, *3*, 385.

[13] T. Kato, J. M. J. Fréchet, P. G. Wilson, T. Saito, T. Uryu, A. Fujishima, C. Jin, F. Kaneuchi, *Chem. Mater.* **1993**, *5*, 1094, and ref. cit. therein.

[14] R. Deschenaux, I. Kosztics, B. Nicolet, *J. Mater. Chem.* **1995**, *5*, 2291.

[15] A.-M. Levelut, J. Malthête, C. Destrade, H.-T. Nguyen, *Liq. Cryst.* **1987**, *2*, 877.

[16] C. M. Paleos, D. Tsiourvas, *Angew. Chem.* **1995**, *107*, 1839; *ibid.*, *Int. Ed. Engl.* **1995**, *34*, 1696; T. Kato, J. M. J. Fréchet, *Macromol. Symp.* **1995**, *98*, 311.

Received August 5, 1998